Journal of Medicinal Chemistry

Article

Design, Synthesis, and Biological Evaluation of New 1-(Aryl-1H-pyrrolyl)(phenyl)methyl-1H-imidazole Derivatives as Antiprotozoal Agents

Francesco Saccoliti, Valentina Noemi Madia, Valeria Tudino, Alessandro De Leo, Luca Pescatori, Antonella Messore, Daniela De Vita, Luigi Scipione, Reto Brun, Marcel Kaiser, Pascal Mäser, Claudia Magalhaes Calvet Alvarez, Gareth K Jennings, Larissa M. Podust, Giacomo Pepe, Roberto Cirilli, Cristina Faggi, Annalise Di Marco, Maria Rosaria Battista, Vincenzo Summa, Roberta Costi, and Roberto Di Santo

J. Med. Chem., **Just Accepted Manuscript** • Publication Date (Web): 07 Jan 2019

ACS Publications

is published by the American Chemical Society. 1155 Sixteenth Street N.W., Washington, DC 20036

Design, Synthesis, and Biological Evaluation of New 1-(Aryl-1*H*-pyrrolyl)(phenyl)methyl-1*H*-imidazole Derivatives as Antiprotozoal Agents

Francesco Saccoliti,[a] Valentina Noemi Madia,[a] Valeria Tudino,[a] Alessandro De Leo,[a] Luca Pescatori,[a] Antonella Messore,[a] Daniela De Vita,[a] Luigi Scipione,[a] Reto Brun,[b] Marcel Kaiser,[b] Pascal Mäser,[b] Claudia M. Calvet,[c, d] Gareth K. Jennings,[c] Larissa M. Podust,[c] Giacomo Pepe,[e] Roberto Cirilli,[f] Cristina Faggi,[g] Annalise Di Marco,[h] Maria Rosaria Battista,[h] Vincenzo Summa,[h] Roberta Costi,[a,] Roberto Di Santo.[a]*

[a] Istituto Pasteur-Fondazione Cenci Bolognetti, Dipartimento di Chimica e Tecnologie del Farmaco, "Sapienza" Università di Roma, p. le Aldo Moro 5, I-00185 Rome, Italy.

[b] Swiss Tropical and Public Health Institute, Socinstrasse 57, CH-4002 Basel, Switzerland

[c] Skaggs School of Pharmacy and Pharmaceutical Sciences, University of California San Diego, La Jolla, California 92093, USA

[d] Laboratório de Ultraestrutura Celular, Instituto Oswaldo Cruz (IOC), FIOCRUZ, Rio de Janeiro, Rio de Janeiro, Brazil, 21040-360

[e] Dipartimento di Farmacia, Università di Salerno, Via Giovanni Paolo II 132, I-84084 Fisciano, Salerno, Italy

[f] Centro Nazionale per il Controllo e la Valutazione dei Farmaci, Istituto Superiore di Sanita', Viale Regina Elena 299, I-00161 Rome Italy

[g] Dipartimento di Chimica, Università degli studi di Firenze, Via della Lastruccia 13, I-50019 Sesto Fiorentino, Florence, Italy

[h] Drug Discovery, IRBM Science Park, Via Pontina km 30,600, 00071 Pomezia, Rome, Italy

ABSTRACT: We have designed and synthesized a series of new imidazole-based compounds structurally related to an antiprotozoal agent with nanomolar activity which we identified recently. The new analogs possess micromolar activities against *T. b. rhodesiense* and *L. donovani* and nanomolar potency against *P. falciparum.* Most of the analogs displayed the IC_{50} within the low nanomolar range against *T. cruzi*, with very high selectivity towards the parasite. Discussion of structure-activity relationships and *in vitro* biological data for the new compounds are provided against a number of different protozoa. The mechanism of action for the most potent derivatives (**5i, 6a-c, 8b**) was assessed by a target-based assays using recombinant *T. cruzi* CYP51. Bioavailability and efficacy of selected hits was assessed in a *T. cruzi* mouse model, where **6a** and **6b** reduced parasitemia in animals >99% following intraperitoneal administration of 25 mg/kg/day dose for four consecutive days.

INTRODUCTION

Plasmodium and trypanosomatid parasites cause vector-borne infections producing a great deal of chronic diseases and affecting hundreds of millions people mainly in developing countries. However, in the last years, due to several factors including vector and human migrations or co-infections in immunosuppressed patients, such diseases are dramatically spreading worldwide.[1] Malaria is the most challenging and deadly parasitic disease since nearly half of the world's population is at risk of being infected with roughly 216 million cases and an estimated 445.000 deaths in 2016. Among the five species of *Plasmodium* parasites causing human disease, *P. falciparum* is the most deadly.[2] Human trypanosomatid diseases, including leishmaniasis, Chagas disease and human African trypanosomiasis (HAT), are classified by WHO as the most challenging among the Neglected Tropical Diseases since they cause morbidity and mortality mainly in tropical and sub-tropical countries hindering their economic development.[3,4] Due to economic reasons, they do not represent an attractive market for pharmaceutical companies which sharply contrasts with the disproportional number of people at risk, affected patients and related fatalities.[5,6] Human trypanosomatid infections are becoming a severe global health concern affecting more than 20 million people.[7] Parasites of the genus *Leishmania*

cause three main forms of leishmaniasis, with the visceral form (VL) being life-threatening and the second most deadly parasitic disease. Estimated numbers of VL cases are 700.000-1 million new cases per year, with approximately 30.000 deaths each year, although it is not often recognized or reported.[8,9] Chagas disease is caused by *Trypanosoma cruzi* representing a major cause of morbidity and mortality in Latin America with as many as 7 million people infected worldwide.[10] *T. brucei gambiense* and *T. brucei rhodesiense* are the causative agents of HAT or sleeping sickness, one of the most complex endemic tropical diseases restricted to Africa.[11]

No vaccines are available and the current antiprotozoal therapies are unsatisfactory due to their low efficacy (especially in the late stage disease), high toxicity and due to the appearance of resistant parasitic strains. Therefore, there is an urgent need to develop new effective, safe and affordable antiprotozoal drugs.[1,3,9,12,13]

Azole-based compounds are known effective antifungal agents targeting sterol 14α-demethylase (CYP51), a pivotal enzyme involved in ergosterol biosynthesis representing the major component of fungal cytoplasmic membranes and playing both structural and functional roles.[14,15] This enzyme is a member of the cytochrome P450 superfamily (CYP51), catalyzing oxidative removal of the 14α -methyl group from post-squalene sterol precursors. Similar to fungi, trypanosomatid parasites also

produce ergosterol and ergosterol-like molecules which are essential for membrane functioning in parasite growth, development and division.[15,16] Via drug repurposing strategy, antifungal azole drugs showed promising antileishmanial and anti-*T. cruzi* activities with miconazole (**1**) being the first antifungal agent tested against *T. cruzi* showing potent growth inhibition.[15,17-20] Experimental CYP51 inhibitors have been developed that demonstrated encouraging results in both *in vitro* and *in vivo* models.[7,15,17,21-31] Recently, the triazole drugs posaconazole (**2**) and ravuconazole (**3**) (Figure 1) were tested in clinical trials for Chagas disease.[15,17,32a-c] Based on the positive PCR read-out, 70-80% treatment failure was reported.[32d,e] Inferiority of both CYP51 inhibitors to benznidazole (Bz) in these clinical trials put on hold development of the azole inhibitors for the treatment of diseases caused by protozoan parasites.[32e,f]

In support of the CYP51 target, the limited efficacy and lack of translation from *in vitro* and *in vivo* models was attributed to the short duration of treatment and sub-optimal doses administered during human clinical trials. Particularly, it has been argued that the dose employed in clinical trials corresponded to only the 10-20% of the curative dose in mice. The short follow-up time did not permit the evaluation of the long-term effects and assessment of clinical symptoms. Due to the pivotal role

played by CYP51 in *T. cruzi* and *Leishmania* spp. biology, it is critical not to reject this drug target before investigating CYP51 utility for the treatment of both acute and chronic Chagas disease in more details.[15,23,25,32g-i] These considerations drive our search for new CYP51 inhibitors with pharmacological properties, high efficacy and low toxicity, making them amenable for long-term administration.[7,15,23-25]

Recently, we evaluated the anti-trypanosomatid and antiplasmodial activities of our in-house antifungal 1-[(aryl)(4-aryl-1*H*-pyrrol-3-yl)methyl]-1*H*-imidazole and 1-(phenyl(1-phenyl-1*H*-pyrrol-3-yl)methyl)-1*H*-imidazole derivatives, with the former compounds being endowed with higher potency against *T. cruzi* and *P. falciparum*.[33a-h,34]

The most promising compounds proved to inhibit *T. cruzi* CYP51 (TcCYP51) in an orthogonal target-based assay. On the other hand, given that *P. falciparum* lacks a steroidogenic pathway, inhibition of *P. falciparum* was via yet unknown target. Among them, derivative **RDS 416** (**4**) (Figure 2) proved to be one of the most promising compounds, showing nanomolar anti-*T. cruzi* activity, submicromolar antiplasmodial activity and micromolar activity against *L. donovani* and *T. brucei*. *In vitro*, **4** was two orders of magnitude more active than the reference drug Bz and also displayed high selectivity towards *T. cruzi* (SI = 275).

In this work, starting from the promising scaffold **4**, we designed and synthesized the new imidazole derivatives **5a-l**, **6a-c, 7a-f** and **8a-c** (Figure 2), with the aim of improving the structure-activity relationships (SARs) within this new class of antiprotozoal compounds. In particular, we designed 1-[(aryl)(4-aryl-1*H*-pyrrol-3-yl)methyl]-1*H*-imidazoles **5a-l** and 1-(phenyl(1-phenyl-1*H*-pyrrol-3-yl)methyl)-1*H*-imidazoles **7a-f**, as derivatives of the recently discovered 1-[(aryl)(1(or 4)-aryl-1*H*-pyrrol-3-yl)methyl]-1*H*-imidazoles related to **4.** Moreover, we decided to further study the effect of the position of the phenyl substituent on the pyrrole ring by designing 1-(phenyl(5-phenyl-1*H*-pyrrol-3-yl)methyl)-1*H*-imidazoles **6a-c** and 1-(phenyl(1-phenyl-1*H*-pyrrol-2-yl)methyl)-1*H*-imidazoles **8a-c**.

Furthermore, the racemic mixture of **4**, that was one of the most potent antiprotozoal compounds previously identified by us, was separated by HPLC on chiral stationary phase to obtain single enantiomers (+)-**4** and (-)-**4**. The enantiomers were characterized and separately tested against protozoa to define the effect of the chiral center on the antiprotozoal activities.

Thus, the newly synthesized derivatives **5a-l, 6a-c, 7a-f, 8a-c** and the enantiomers (+)-**4** and (-)-**4** were tested against the kinetoplastids *T. cruzi*, *L. donovani* and *T. b.*

rhodesiense, and the apicomplexan *P. falciparum*, in order to evaluate their antiprotozoal activities and analyze their SARs.

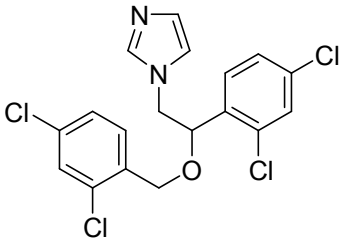

MICONAZOLE (1)

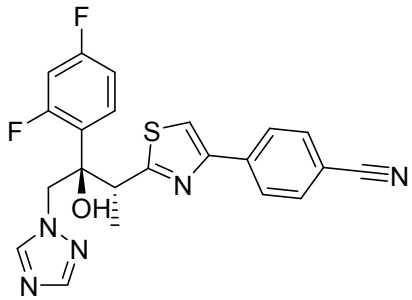

RAVUCONAZOLE (2)

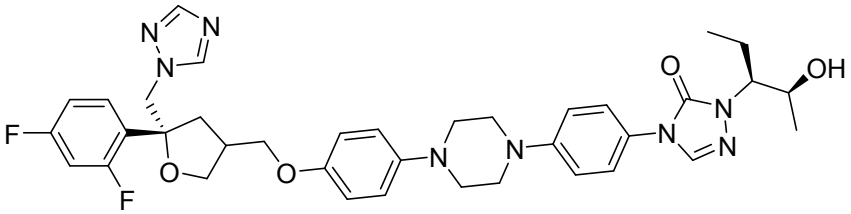

POSACONAZOLE (3)

Figure 1. Chemical structures of some azole antifungal agents displaying antiprotozoal activities.

Derivatives **5a-l, 6a-c, 7a-f**, **8a-c** and the enantiomers (+)-**4** and (-)-**4** displayed potency against the tested parasites in a broad range of concentrations. The highest potencies were achieved by (-)-**4** and **6a-c** against *T. cruzi*. *In vivo* activity of **6a,b** in animal model of *T. cruzi* infection was also demonstrated. The orthogonal target-based assay using recombinant target suggested that activity of compounds toward *T. cruzi* was via inhibition of CYP51.

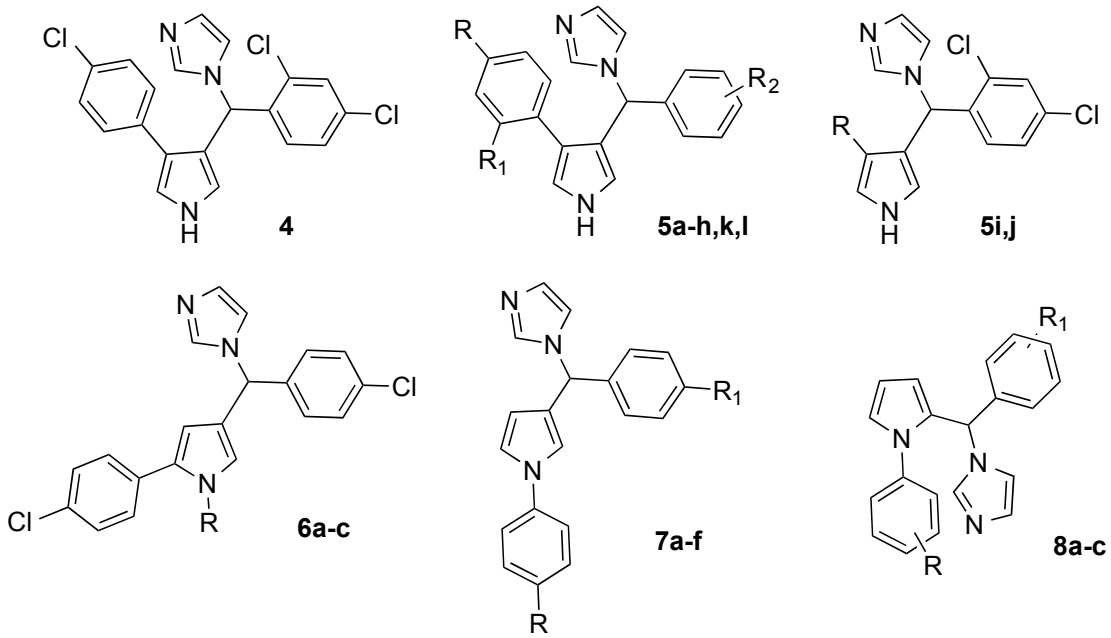

Figure 2. Structures of the reference compound **4** and the new derivatives **5a-l**, **6a-c**, **7a-f** and **8a-c**. For substituents, see Table 1.

RESULTS AND DISCUSSION

Chemistry. The synthesis of the new derivatives **5a-k** is depicted in Schemes 1 and 2, while derivative **5l** has been synthesized as previously reported[33g]. The aldehydes used as starting materials were commercially available (**9a-d,h**) or were synthesized as reported in literature (**9e**,**g,i**)[35-37] with the exception of **9f** that was obtained through a microwave assisted Suzuki reaction of 2,4-dichlorobenzaldehyde with thien-2-yl-boronic acid (Scheme 2). Noteworthy, by means of this procedure, we also obtained by-products **9j** and **9k**. Benzaldehyde **9k** was separated by column chromatography and a mixture of isomers **9f** and **9j** (4:1 ratio) was obtained and employed for the next step.

Compounds **9a-j** underwent a Claisen-Schmidt reaction with the properly substituted acetophenone in the presence of NaOH as base furnishing chalcones **10a,d**[38,39] and **10b,c,e-j** (Scheme 1). Such α,β-unsatured derivatives underwent to ring closure by reacting with toluene-4-sulfonylmethylisocyanide (TosMIC) in the presence of sodium hydride to obtain the corresponding 3-aroylpyrroles **11a-j**. Reduction of the carbonyl group of **11a-j** in the presence of lithium aluminum hydride furnished the corresponding alcohols **12a-j**, which were reacted with *N,N'*-carbonyldiimidazole (CDI) to afford the final imidazoles **5a-j**. Finally, the sulfone derivative **5k** was obtained by oxidation with oxone of the already reported imidazole **5l**[33g,34] .

Scheme 1. Synthetic Route to **5a-k** Derivatives[a]

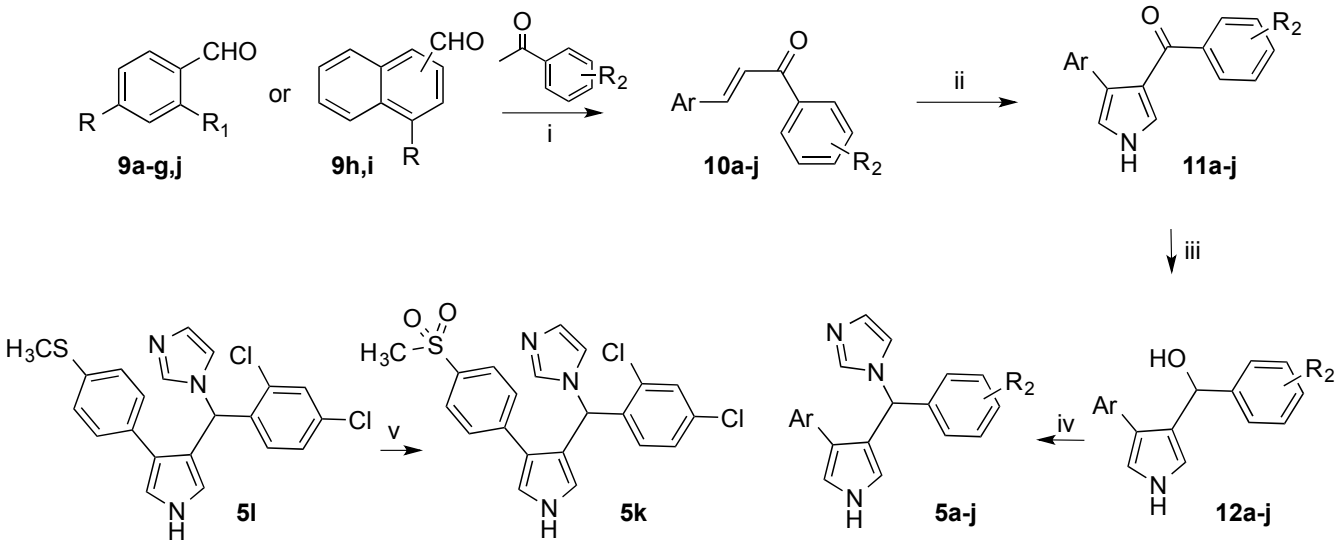

[a] Reagents and conditions: (i) NaOH, EtOH, room temp, 15 h, 50-100 % yield; (ii) TosMIC, NaH, DMSO, Et_2O, room temp, 15-60 min, 18-85% yield; (iii) $LiAlH_4$, THF, 0 °C to room temp, 30 min-3 h, 96-100 % yield; (iv) CDI, CH_3CN dry, room temp, 45 min-20 h, 24-100 % yield; (v) oxone, H_2O, MeOH, 0 °C to room temp, 18 h, 100 % yield. For substituents, see Table S1 in Supporting Information.

Scheme 2. Synthetic Route to **9f** Derivative[a]

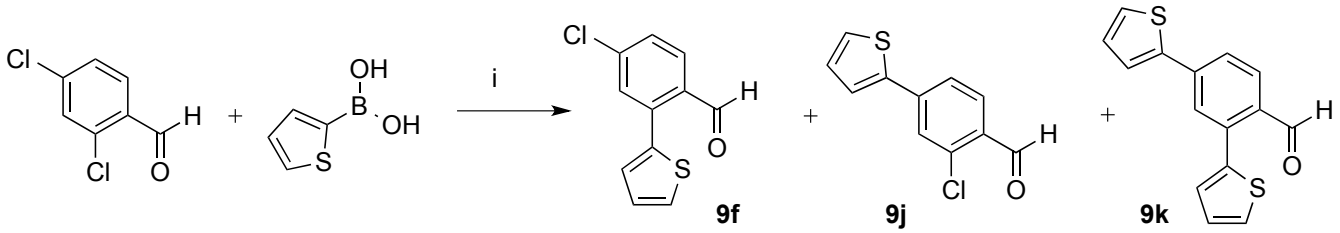

[a] Reagents and conditions: (i) $Pd(dba)_2/PCy_3$, $K_2PO_4 \cdot H_2O$, DMF, 100 W, 100 psi, 80 °C, 1 h, 44 % (**9f**), 11 % (**9j**), 21 % (**9k**) yields.

Azoles **6a-c** were synthesized as reported in Scheme 3. The preparation of the crucial intermediate **14** was achieved by cycloaddition of isocyanide **13** with 3-chloro-1-(4-chlorophenyl)propan-1-one in the presence of NaH. The pyrrole **14** that formed was alkylated by reaction with the appropriate alkyl halide in the presence of K_2CO_3 to obtain *N*-alkylpyrroles **15b,c**. The methanones **14** and **15b**,**c** were then reduced to the corresponding alcohols **16a-c**, which underwent to reaction with CDI to give imidazoles **6a-c**.

Scheme 3. Synthetic Route to **6a-c** Derivatives[a]

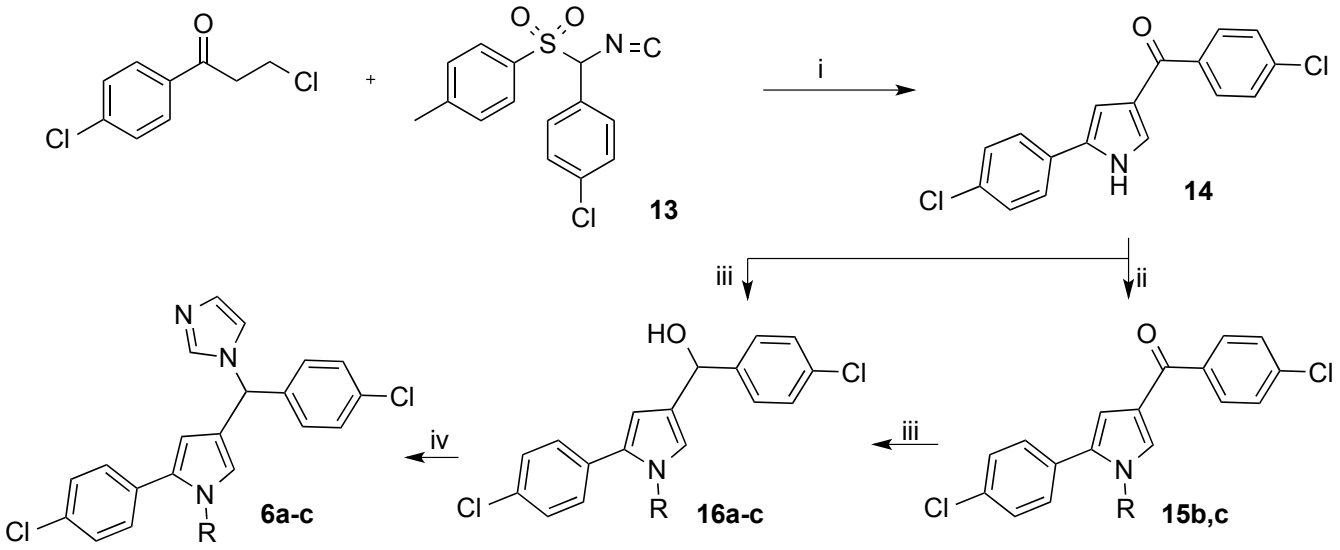

[a] Reagents and conditions: (i) NaH, DMSO, Et_2O, room temp, 50 min, 33 % yield; (ii) proper alkyl halide, K_2CO_3, DMF, 90 °C, 3.5-54 h, 44-92 % yield; (iii) $NaBH_4$, THF, room temp or reflux, 4.5-23 h, 100 % yield; (iv) CDI, CH_3CN dry, room temp, 80 min-15 h, 67-82 % yield. For substituents, see Table S1 in Supporting Information.

The known intermediate **13** necessary as the starting material was prepared according to Scheme 4 through a procedure modified with respect of the one already reported in the literature[40] achieving high yields in shorter reaction times. In particular, compound **13** was prepared by a Mannich reaction of formamide with *p*-toluenesulfinic acid and 4-chlorobenzaldeheyde in the presence of trimethylsilyl chloride (TMSCl) to give *N*-[(4-chlorophenyl)(tosyl)methyl]formamide[40] (**17**) that was then dehydrated by reaction with $POCl_3$ and Et_3N at -10 °C for 45 min.

Scheme 4. Synthetic Route to **13** Derivative[a]

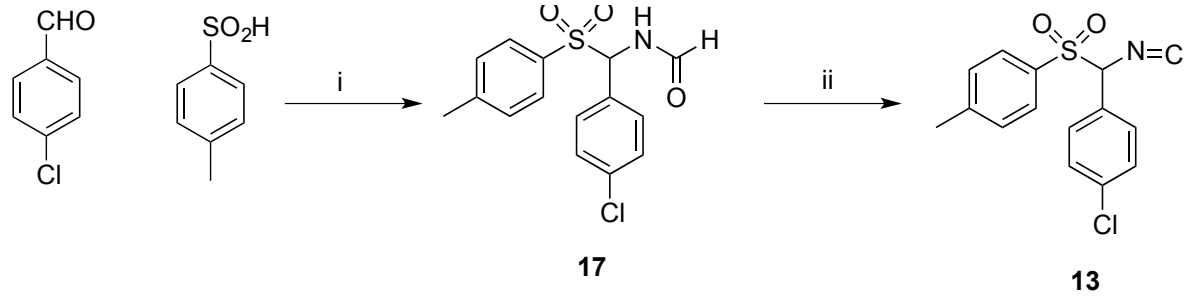

[a] Reagents and conditions: (i) formamide, TMSCl, toluene, CH_3CN, 50 °C, 5 h, 80 % yield; (ii) $POCl_3$, Et_3N, DME, -10 °C, 45 min, 91 % yield.

The synthetic pathway to obtain derivatives **7a-f** and **8a-c** is reported in Scheme 5. The *N*-phenylpyrroles **18a-e**[41-43] underwent a Friedel-Craft acylation in the presence of the properly substituted benzoyl chloride to give mixture of α- and β-isomers **19a-c** and **20a-f**, respectively, that were separated by column chromatography. After separation, ketones **19a-c** and **20a-f** were reduced with $NaBH_4$ to

alcohols **21a-c** and **22a-f**, that were then reacted with CDI to obtain the imidazole derivatives **7a-f** and **8a-c**.

Scheme 5. Synthetic Route to **7a-f** and **8a-c** Derivatives[a]

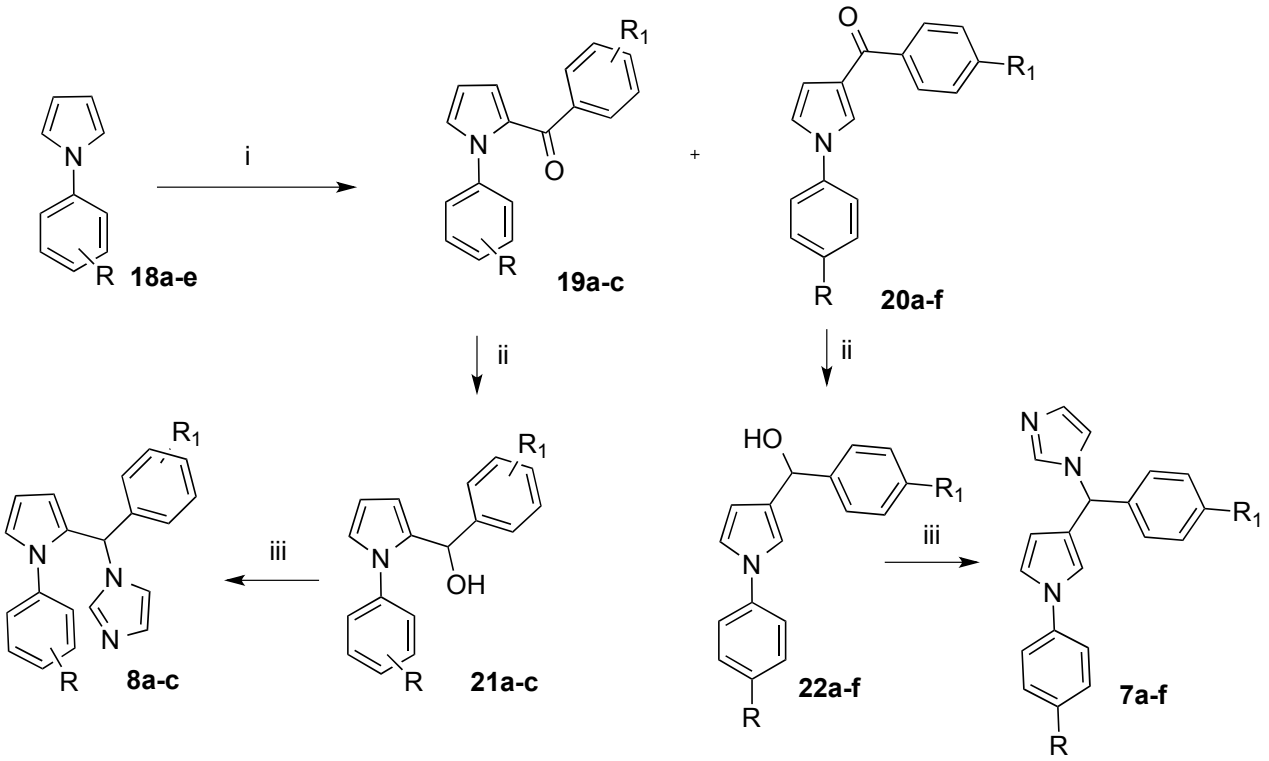

[a] Reagents and conditions: (i) substituted benzoyl chloride, $AlCl_3$, DCM, room temp, 15 h, 4-21 % yield; (ii) $NaBH_4$, THF, room temp or reflux, 2.5-48 h, 88-100 % yield; (iii) CDI, CH_3CN dry, room temp 40 min-15 h, 20-100 % yield. For substituents, see Table S1 in Supporting Information.

Enantiomeric Separation of Racemic Mixture of 4. Racemate **4** was chosen to perform an enantiomeric separation of the single enantiomers generated by the stereogenic center that characterizes these series of antiprotozoal agents. Accurate semipreparative enantioselective HPLC of racemate **4** was carried out on the Chiralcel OD chiral stationary phase (CSP) and enabled us to isolate tens of mg of enantiopure samples of (-)-**4** and (+)-**4**, in 90% isolation yields. The enantiomeric purity of the collected enantiomers (-)-**4** and (+)-**4** was checked and demonstrated both by analytical HPLC and polarimetric

and circular dichroism (CD) analysis. As shown in Figure 3, the chiroptical properties of the enantiopure antipodes isolated on mg-scale were perfectly specular.

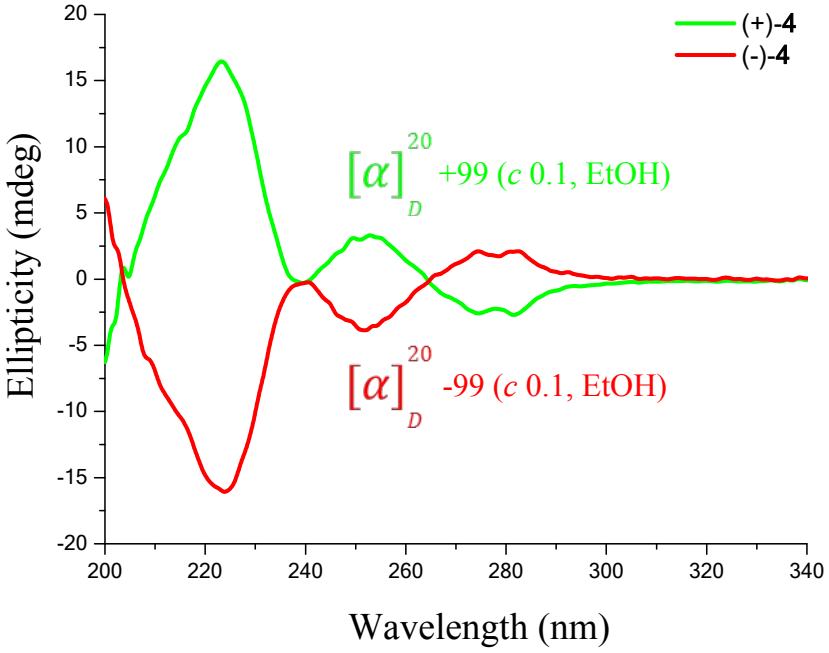

Figure 3. CD spectra and specific rotations of the enantiomers (-)-**4** and (+)-**4** recorded in ethanol.

The absolute configuration of the (-)-**4** (second eluted enantiomer on the Chiralcel OD CSP using the mixture 70:30 *n*-hexane/EtOH as a mobile phase) was unequivocally determined by X-ray analysis. Suitable crystals of the enantiomer were obtained by crystallization from methanol/water. An ORTEP view of (*R*)-(-)-**4** is illustrated in Figure 4.

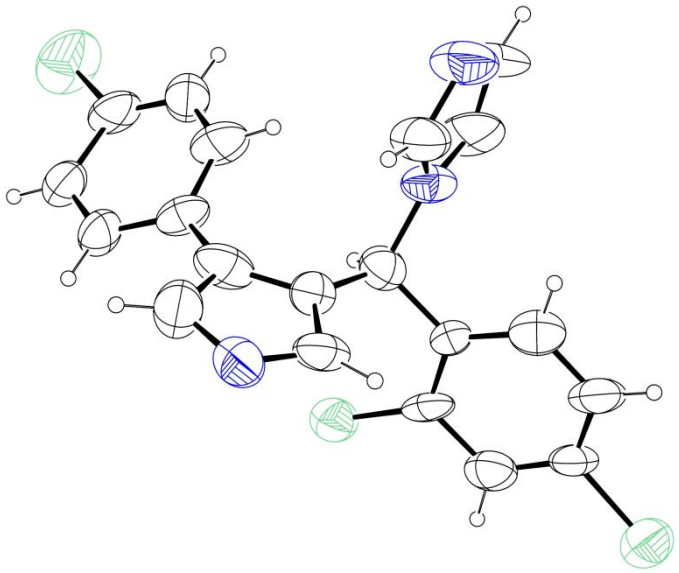

Figure 4. An ORTEP view of the molecular structure of (*R*)-(-)-**4**.

Evaluation of Biological Activities. *In vitro phenotypic studies.* All the newly designed and synthesized derivatives **5a-k**, **6a-c**, **7a-f** and **8a-c** were tested against *T. cruzi* amastigotes, *L. donovani* axenic amastigotes, *T. b. rhodesiense* trypomastigotes and apicomplexan *P. falciparum* blood stage forms.

The results are reported in Table 1. The compounds showed anti-*T. cruzi* and antiplasmodial activities within the submicromolar and nanomolar range, proving to be also able in inhibiting *L. donovani* and *T. b. rhodesiense* at micromolar concentration.

Due to these different ranges, the *in vitro* activities as well as the SARs of the imidazole-based compounds **5a-k**, **6a-c**, **7a-f** and **8a-c** will be discussed separately for each parasite.

Although most compounds exhibit a certain cytotoxicity, many of them displayed high to very high selectivity towards *T. cruzi*, showing IC_{50} values within the nanomolar range and SI > 100. Additionally, four compounds showed selective submicromolar-nanomolar inhibitory potencies against *P. falciparum* parasite.

In vitro activity against Trypanosoma brucei and Leishmania donovani. The tested imidazole derivatives **5a-k**, **6a-c**, **7a-f** and **8a-c** displayed lower activities against *T. b. rhodesiense* and *L. donovani* compared to their anti-*T. cruzi* and antiplasmodial activities, according to the trend previously described by us for 3-arylpyrrole derivative **4** and congeners[34].

In fact, **5a-k**, **6a-c**, **7a-f** and **8a-c** showed micromolar IC_{50} values in the range 7.39 - 89.25 μM on the trypomastigote bloodstream form of *T. b. rhodesiense* with SI ranging from 1 to 13. Only two compounds (**5f, 6a**) highlighted IC_{50} < 10μM with the α-phenyl pyrrole compound **6a** being the most active (**6a**, IC_{50} = 7.39 μM) but about 800 times less active than the reference drug (MEL).

Otherwise, the newly synthesized derivatives displayed higher inhibitory potencies against axenic *L. donovani* amastigotes compared to *T. b. rhodesiense*, showing IC_{50} in the range 2.04 - 84.43 μM and SI ranging from 1 to 9. Notably, more than 50% of the tested compounds showed IC_{50} < 10 μM, with the tetrachloro derivative **8c** being the most active (**8c**, IC_{50} = 2.04 μM), about 4 times less potent than reference drug MF.

In vitro activity against Plasmodium falciparum. Although *P. falciparum* does not have sterol biosynthesis pathway neither CYP51, we investigated the antiplasmodial activities of the compounds since some azole derivatives have been reported in the literature as promising antimalarial agents.[44-48] Moreover, according to this, we recently reported a series of imidazole-based compounds endowed with notable antiplasmodial potencies within the submicromolar range.[34]

The biological evaluation on the erythrocytic stage of *P. falciparum* gave from good to excellent results since the tested derivatives were active in the range 0.059-4.99 μM with SI ranging from 9 to 253.

Among the 23 newly synthesized compounds, 14 (61%) displayed submicromolar or nanomolar antiplasmodial activities, whereas the remaining 9 showed IC_{50} in the low micromolar range ($IC_{50} < 5$ μM). In particular, 11 out of 14 derivatives (**5a-d,f,i,j, 6a,c, 8a,b**) resulted active at submicromolar concentrations whereas 3 of them (**5g,h, 8c**) highlighted nanomolar potencies, proving to be up to 3 times more active than the reference drug chloroquine (CHQ). On the other hand, none of the new compounds resulted more active than artemisinin (ART).

It is noteworthy that the antiplasmodial activities are well correlated with the intramolecular distance between the benzyl-imidazolyl moiety and the phenyl ring bound to the pyrrole core. In fact, it seems that the higher is the gap (1,3-relative positions) the lower are the inhibitory potencies. According to this, derivatives of series **6** and **7**, displaying micromolar or high submicromolar inhibitory potencies, resulted less active than 1,2-substituted series **5** and **8** which are endowed with submicromolar up to nanomolar potencies. Interestingly, 1-(phenyl(1-phenyl-1*H*-pyrrol-3-yl)methyl)-1*H*-imidazole derivatives (**7a-f**) proved to be the less encouraging antiplasmodial compounds of the series, according to the trend we described previously.[34]

The chlorine atom in 4-position of the phenyl ring linked to the pyrrole core of **4** was replaced with alkyl, methoxy, thiomethyl and methylsulphonyl groups, leading to derivatives **5a-d,l**. These compounds were comparable or less active than the parent compound **4**. In particular, we observed activities decreasing in the following order: $SCH_3 > CH(CH_3)_2 > CH_3 > C_2H_5 > OCH_3 > SO_2CH_3$. The most active compounds **5a**, **5b**, **5c** and **5l** (IC_{50} = 0.29 μM; IC_{50} = 0.30 μM; IC_{50} = 0.28 μM; IC_{50} = 0.24 μM, respectively) were derivatives characterized by lipophilic groups. Conversely, the replacement of methyl with methoxy or methylthio with methylsulphonyl moieties gave more polar derivatives endowed with decreased activities (compare **5a** with **5d** and **5l** with **5k**, respectively). This trend is respected comparing the more polar methoxy derivative **5d** (IC_{50} = 0.46 μM) with the more lipophilic isoster **5l** (IC_{50} = 0.24 μM).

The introduction of an aryl or heteroaryl substituents in 2'-position of the 4-phenyl group linked to the pyrrole ring of **4** proved to be a useful approach. In fact, although the introduction of a pyrrole group gave compound **5e** that was 28 times less potent than the parent compound (IC_{50} = 4.53 μM *vs* IC_{50} = 0.16 μM, respectively), the introduction of a 2-thienyl or phenyl rings gave very good results. In fact, the thienyl derivative **5f** was active at submicromolar concentration (IC_{50} = 0.27 μM) resulting comparable to **4,** and even more, the phenyl derivative **5g** (IC_{50} = 96 nM) was 3 times more potent than **5e** and also 2 times more active than CHQ and the reference compound **4.**

Very interestingly, the removal of the 2-chloro substituent from the 3-(2,4-dichlorophenylmethylimidazole) moiety of the trichloro derivative **5g** led to the dichloro counterpart **5h** that showed an increased activity if compared to the parent compound (IC_{50} = 59 nM *vs* IC_{50} = 96 nM) resulting 2 times more active than **5g** and 3 times more potent than the reference azole **4**. It is worthy to note that compound **5h** proved to be the best antiplasmodial compound of this series resulting 3 times more active than CHQ (IC_{50} = 59 nM *vs* IC_{50} = 0.174 μM).

Finally, the replacement of the 4-phenyl ring linked to position 4 of the pyrrole core of **4** with naphthyl groups was exploited. In particular, the introduction of a 2-naphthyl and 4-chloro-1-naphthyl

led to derivatives **5i**, and **5j** which showed IC_{50} = 0.34 μM and IC_{50} = 0.33 μM, respectively, that were 2 times less active than **4**.

Excellent antiplasmodial activities have been highlighted by *N*-phenyl pyrroles **8a-c**. These compounds are structurally related with derivatives of series **5** and reference compound **4**. In fact, they share a joint geometry between the benzylimidazole moiety and the phenylpyrrole portions, since the last ones have both a 1,2-substitution pattern (Figure 5). Thus, compound **8b** can be directly compared to reference derivative **4**, and very interestingly, these compounds showed similar activity (IC_{50} = 0.18 μM and IC_{50} = 0.16 μM, respectively). The replacement of the 2,4-dichloro substituent of **8b** with a 4-*tert*-butyl group gave derivative **8a** that showed similar activity (IC_{50} = 0.19 μM). It is worthy to note that the introduction of a further chlorine atom in 2' position of the *N*-phenyl ring of the **4** isomer **8b** caused an increase of the inhibitory potency. In particular, the tetrachloro-compound **8c** showed IC_{50} = 80 nM, proving to be 2 times more potent than the parent compound and CHQ.

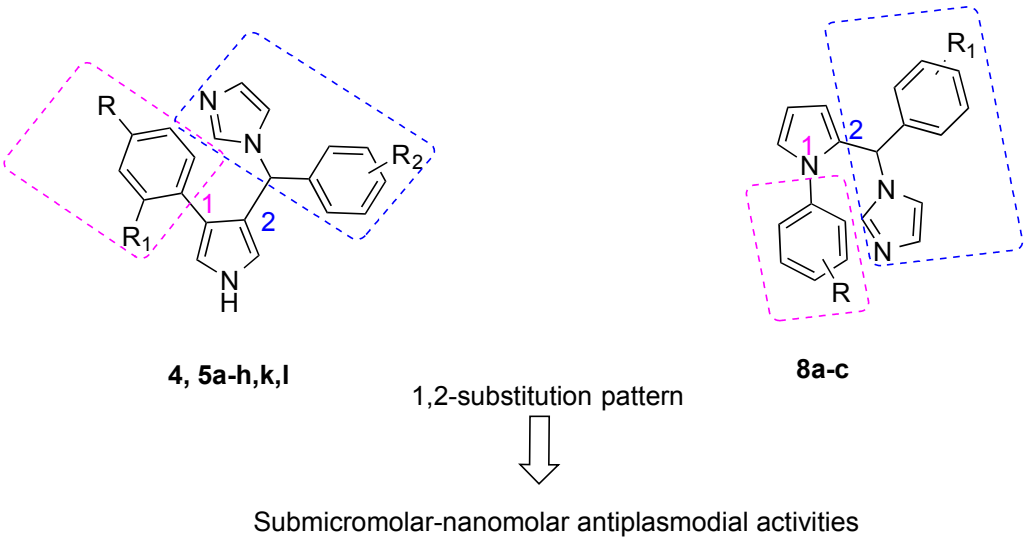

Figure 5. 1,2-Substitution pattern on pyrrole ring and related antiplasmodial activity.

Notably, all the compounds (**5g,h, 8c**) active at nanomolar concentration displayed higher selectivity towards the parasite (SI range, 149-253) compared to the reference compound **4** (SI=60) with the most active derivative **5h** being also the most selective (SI = 253).

Finally, the separation of enantiomers of **4** led to the conclusion that the eutomer in this series of antiplasmodial agent is the R isomer (*R*)-(-)-**4** that showed IC_{50} = 92 nM.

In vitro activity against Trypanosoma cruzi. The biological outcomes on the amastigote form of *T. cruzi* were excellent. In fact, with the exception of derivative **7d**, the newly designed and synthesized azole derivatives proved to be highly active showing IC_{50} in the range 0.002-11.95 μM and SIs ranging from 6 to 4030. Notably, 19 derivatives, representing 86% of the tested compounds, displayed interesting activities with IC_{50} ranging from micromolar to nanomolar concentrations.

In particular, with the exception of **7b, 7c** and **7e** that displayed micromolar activities within the same order of magnitude of Bz used as the reference drug (IC_{50} = 3.60 μM, IC_{50} = 6.18 μM, IC_{50} = 3.90 μM, respectively), the remaining 16 compounds were active at submicromolar and nanomolar concentrations, resulting from one to three orders of magnitude more active than Bz. In particular, three derivatives (**5g, 5h** and **8a**) proved to be active within the submicromolar range resulting 4-12 times more active than Bz (**5g**, IC_{50} = 0.142 μM; **5h**, IC_{50} = 0.203 μM; **8a**, IC_{50} = 0.390 μM), whereas the remaining 13 compounds displayed inhibitory potencies at nanomolar concentrations. In particular, nine derivatives proved to be 25-92 times more active than the reference drug Bz, with derivatives **5f,i,k** being up to 2 times more active than **4** (**5f,** IC_{50} = 27 nM; **5i**, IC_{50} = 18 nM; **5k**, IC_{50} = 29 nM). Finally, the other four compounds (**8b** and **6a-c**) showed excellent anti-*T. cruzi* activities within the low nanomolar range, resulting not only 2-3 order of magnitude (330-825 times) more active than Bz but

also one order of magnitude (7-175 times) more active than the internal reference compound **4** (**6a**, IC_{50} = 3 nM; **6b**, IC_{50} = 3 nM; **6c**, IC_{50} = 2 nM; **8b**, IC_{50} = 5 nM).

Notably, all the submicromolar/nanomolar active compounds displayed high or very high selectivity against the parasite (SI range, 74-4030). In particular, derivatives showing inhibitory potencies at low nanomolar concentrations highlighted SI > 2000, thus being far more selective than **4**.

With the exception of derivative **5e**, all the analogues of **4** (**5a-d,f-l**) displayed good submicrolar-nanomolar activities highlighting also high selectivity against the parasite.

The replacement of the 4'-chlorine atom of **4** with methyl, ethyl, isopropyl, thiomethyl, methylsulfonyl or methoxy substituents led to derivatives **5a-d,k,l** active at nanomolar concentration. In particular, **5a**, **5b, 5c 5d**, and **5l**, showed IC_{50} in the range 43-66 nM, while **5k**, was the most potent within this group with IC_{50} = 9 nM and proved to be 57 times more potent than Bz. It is worthy to note that, contrary to what has been observed for *P. falciparum*, the oxidation of the methylsulphide group of **5l** into the corresponding methylsulphone led to the more potent derivative **5k**, which resulted also more active than reference **4**. In the end, it is possible to observe that the activity can be described in the following order SO_2Me > Cl > SMe > OMe > *i*-Pr > Et (**5k** > **4** > **5l** > **5d** > **5a** > **5b**,**c**).

The introduction of an aryl or heteroaryl group in position 2 of the phenyl ring linked to the pyrrole core on the 4-phenyl ring of **4** led to derivatives **5e-h** endowed with a wider range of activities. In fact, depending on the nature of the (hetero)aryl substituent, the inhibitory potencies ranged from micromolar to nanomolar concentrations.

In particular, the introduction of a 1-pyrrolyl group caused a substantial decrease of activity since compound **5e** resulted nearly 340 times less active than the reference compound **4** being also one order of magnitude less active than Bz (IC_{50} = 11.95 μM). On the contrary, the introduction of a phenyl group in that position led to compounds active at submicromolar concentration. In particular, both biphenyl derivatives **5g,h** proved one order of magnitude more active than Bz and 4-6 times less potent than the reference compound **4** (**5g**, IC_{50} = 0.142 μM; **5h**, IC_{50} = 0.203 μM). Notably, the trichloro derivative **5g** was more active than the dichloro counterpart **5g**.

Finally, the introduction of a 2-thienyl substituent on the phenyl linked to the pyrrole moiety led to compound **5f** that proved active at nanomolar concentration (IC_{50} = 27 nM), was 61 times more active than Bz and also slightly more potent than **4.**

Thus, concerning the nature of the 2'-substituent linked to the 4-phenyl ring of **4** analogues it is possible to observe that the activity has the following order: 2-thienyl > H > Ph >> 1-pyrrolyl (**5f** > **4** > **5g** >> **5e**).

Finally, the replacement of the 4-phenyl ring of **4** with naphthyl groups led to compounds active at nanomolar concentrations. In particular, the introduction of a 4-chloro-1-naphthyl group (**5j**) caused a slight decrease of the inhibitory potency (IC_{50} = 48 nM). On the contrary, the replacement with a 2-naphthyl moiety led to derivative **5i**, which showed very good activity (IC_{50} = 18 nM). Notably, this compound resulted 2 times more active than **4**, proving to be also the most active anti-*T. cruzi* derivative of series **5**.

The shift of the phenyl ring of compounds of series **5** from position 4 to the positions 5 and 1 of the pyrrole core, led to phenyl pyrroles of series **6** and **7**, respectively. Concerning the compounds of series **7**, we obtained derivatives endowed with micromolar inhibitory potencies against *T. cruzi*, with the exception of **7d,** which was inactive. In particular, **7a-c**,**e**,**f** proved to be from 2 to 6 times less active than Bz displaying SI values ranging from 6 to 44. Among them, the most active compound was the dinitro derivative **7b**, which showed a nearly 2 times lower anti-*T. cruzi* activity in respect of Bz proving to be also the most selective compound of this group (IC_{50} = 3.60 μM; SI = 44).

Generally, among the newly designed and synthesized azoles, 1-(phenyl(1-phenyl-1*H*-pyrrol-3-yl)methyl)-1*H*-imidazole derivatives **7a-e** proved to be endowed with the lowest inhibitory potencies and selectivity, confirming the trend previously described by us.[34]

Conversely, the α-phenyl pyrroles **6a-c**, obtained by shifting the 4-phenyl ring of **4** from position 4- to position 5- of the pyrrole moiety, showed excellent potencies against *T. cruzi*. In fact, derivatives **6a-c** proved to be active within the low nanomolar range and presented the best anti-*T. cruzi* activities among the newly synthesized antiprotozoal agents. They are 550-825 times more active than Bz and 12-18

times more potent than the internal reference compound **4**. The selectivity of these agents was also very good since **6a-c** showed SIs values ranging from 2217 to 4030, resulting 8-15 times more selective than **4**.

The substituent on the pyrrole nitrogen seems not to influence the activity of these compounds. In fact, derivatives **6a,b** showed the same anti-*T. cruzi* activities (**6a**,**b**, IC_{50} = 3 nM), suggesting that the presence of an hydrogen or a methyl group in such position does not affect the antiprotozoal activity. Further, the *N*-alkylation of the nitrogen pyrrole with an allyl group gave **6c** that was just slightly more effective than compounds **6a** and **6b**, with a nearly 2-times improvement of the inhibitory potency. However, it is worthy to note that among the azole compounds described, derivative **6c** was the most active one, highlighting an IC_{50} of 2 nM. Notably, this derivative proved to be 825 times more potent than Bz, and 18 times more active than **4** showing also a very high selectivity towards the *T. cruzi* parasite (SI = 3880).

A further shift of the phenyl ring was realized obtaining *N*-phenyl pyrroles **8a-c.** These compounds are isomers of derivatives **7** but are strictly related to azoles of series **5** since the relative position of the benzylimidazole moiety and the phenyl ring is 1,2 in both cases.

Derivatives **8a-c** highlighted inhibitory potencies at submicromolar up to nanomolar concentrations, resulting from 4 to 330 times more active than Bz and showing also high selectivity towards the parasite with SI values ranging from 119 to 2776.

Since **8b** and **4** have the same substituents and also the same geometry, a direct comparison can be addressed. Noteworthy **8a** displayed excellent inhibitory potency and resulted the most active and selective compound of the **8** series (IC_{50} = 5 nM, SI = 2776), proving to be not only 3 orders of magnitude more active than Bz but also 7 times more active than **4**. The replacement of the chlorine atom linked to the *N*-phenyl group with a *tert*-butyl substituent, gave derivative **8a,** which showed a decrease in activity (IC_{50} = 0.39 μM) if compared to both the parent compound **8b** and **4**. In fact, although it resulted 4 times more potent than Bz, it resulted 11 times less active than **4** being also endowed with 2 order of magnitude lower potency in respect of derivative **8b**. Conversely, the

introduction of a further chlorine atom in 2' position of the *N*-phenyl moiety of **8b** led to compound **8c,** which, although active at nanomolar concentration, resulted less active than the parent compound**.** In particular, **8c** (IC_{50} = 62 nM) was 27 times more active than Bz, 2 times less active than **4** and 12 times less potent than **8b**.

In vitro activity of enantiomers of compound 4. Finally, separated enantiomers of the potent reference derivative **4** have been tested against the protozoa panel.

(*S*)-(+)-**4** isomer displayed higher activity against *T. b. rhodesiense* and comparable antileishmanial potency in respect of the racemate **4.** Additionally, it displayed promising submicromolar antiplasmodial activity, resulting slightly more active than **4** (**4**, IC_{50} = 0.16 μM; (*S*)-(+)-**4**, IC_{50} = 0.11 μM) and nearly 2 times more potent than CHQ. Further, it showed very good potency against *T. cruzi*, resulting 2 orders of magnitude more potent than Bz and 2 times more potent than the racemate **4** ((*S*)-(+)-**4**, IC_{50} = 17 nM; **4**, IC_{50} = 35 nM).

However, the levorotatory isomer (*R*)-(-)-**4** showed the highest inhibitory potency proving to be the eutomer, being from 2 to 39 times more active than racemate **4** against all parasites. In particular, it resulted 2 times more potent than **4** against *T. b. rhodesiense* and comparable to it against *L. donovani*. Moreover, (*R*)-(-)-**4** showed promising nanomolar potency against *P. falciparum* proving to be 2 times more active than **4** ((*R*)-(-)-**4**, IC_{50} = 92 nM; **4**, IC_{50} = 0.16 μM) and the reference drug CHQ. Finally, it is worthy to note that the eutomer (*R*)-(-)-**4**, showed subnanomolar activity against *T. cruzi*, (IC_{50} = 0.9 nM), being 40 times more active than **4,** 1833 times more potent than Bz and highly selective towards the parasite with SI = 2844.

Table 1. Antiprotozoal activity (*T. b. rhodesiense*, *T. cruzi*, *L. donovani*, and *P. falciparum*) and cytotoxicity of the tested compounds **5a-l**, **6a-c 7a-f** and **8a-c.**

				IC_{50}[a] (μM)								CC_{50}[b] (μM)
Cpds	R	R_1	R_2	Tb[c]	SI[d]	Tc[e]	SI[f]	Ld[g]	SI[h]	Pf[i]	SI[j]	
5a	CH_3	H	2,4-Cl_2	18.83	-	0.050	367	5.64	3	0.29	63	18.36
5b	CH_2CH_3	H	2,4- Cl_2	22.51	-	0.066	202	4.87	3	0.30	45	13.35
5c	$(CH_3)_2CH$	H	2,4- Cl_2	24.22	-	0.066	192	5.22	2	0.28	45	12.70
5d	OCH_3	H	2,4- Cl_2	28.37	-	0.050	296	5.51	3	0.46	32	14.79
5e	Cl	Py[k]	2,4- Cl_2	11.89	-	11.95	-	10.75	-	4.53	2	7.67
5f	Cl	Tioph[l]	2,4- Cl_2	8.31	-	0.027	183	2.78	2	0.27	18	4.93
5g	Cl	Ph[m]	2,4- Cl_2	29.03	-	0.142	101	13.89	1	0.096	149	14.31
5h	Cl	Ph[m]	4-Cl	34.43	-	0.203	74	15.01	-	0.059	253	14.92
5i	2-Np[n]	-	2,4- Cl_2	15.58	-	0.018	363	6.41	1	0.34	19	6.54
5j	4-Cl-1-Np[n]	-	2,4- Cl_2	16.47	-	0.048	102	4.83	1	0.33	15	4.90
5k	SO_2CH_3	H	2,4- Cl_2	33.02	2	0.029	2344	10.15	7	1.30	52	67.98
5l[34]	SCH_3	H	2,4- Cl_2	15.81	-	0.043	168	5.12	1	0.24	30	7.22
6a	H	-	-	7.39	-	0.003	2217	3.01	2	0.78	9	6.65
6b	CH_3	-	-	40.02	-	0.003	4030	5.70	2	1.41	9	12.09
6c	$CH_2CH{=}CH_2$	-	-	38.69	-	0.002	3880	2.16	4	0.63	12	7.76

7a	NO_2	H	-	14.52	4	10.25	6	31.07	2	4.99	12	60.40
7b	NO_2	NO_2	-	11.84	13	3.60	44	17.72	9	2.33	68	158.97
7c	NO_2	Cl	-	40.65	2	6.18	13	25.16	3	4.57	18	82.36
7d	CF_3	Cl	-	31.11	1	>74.66	-	21.28	2	1.81	22	40.07
7e	Cl	CN	-	35.67	1	3.90	11	30.38	1	2.18	19	42.36
7f	CN	CN	-	27.76	5	Dnp[o]	-	84.43	2	4.09	34	139.10
8a	4-Cl	4-^{t}Bu	-	89.25	-	0.39	119	9.54	5	0.19	244	46.42
8b	4-Cl	2,4- Cl_2	-	37.0	-	0.005	2776	5.34	3	0.18	77	13.88
8c	2,4- Cl_2	2,4- Cl_2	-	31.11	-	0.062	149	2.04	5	0.080	116	9.26
4	Cl	H	2,4- Cl_2	17.33	-	0.035	275	3.77	3	0.16	60	9.61
MEL[p]				0.0088	3284.1							28.9
Bz[q]						1.65	>233.3					>385
MF[r]								0.56	244.6			137
CHQ[s]										0.174	533.3	92.8
ART[t]										0.007	>50000	>350
PPT[u]												0.007

[a]Concentration of compound required to decrease parasite viability by 50% compared to the number of parasites grown in the absence of the test compound; [b]Cytotoxicity measurement for L6 cells; [c]*Trypanosoma brucei rhodesiense*, STIB900 trypomastigote; [d]Calculated as (CC_{50})/(IC_{50} for *T.b. rhodesiense*); [e]*Trypanosoma cruzi*, Tulahuen C2C4 amastigote; [f]Calculated as (CC_{50})/(IC_{50} for *T. cruzi*); [g]*Leishmania donovani,* MHOM/ET/67/L82 axenic amastigote; [h]Calculated as (CC_{50})/(IC_{50} for

L. donovani); [i]*Plasmodium falciparum* K1 erythrocytic stage; [j]Calculated as (CC_{50})/(IC_{50} for *P. falciparum*); [k]Py = 1-pyrrolyl; [l]Tioph = 2-thienyl; [m]Ph = phenyl; [n]Np = naphtyl; [o]Determination not possible; [p]melarsoprol; [q]Bz; [r]miltefosine; [s]chloroquine; [t]artemisinin; [u]podophyllotoxin.

Table 2. Antiprotozoal activities (*T. b. rhodesiense*, *T. cruzi*, *L. donovani*, and *P. falciparum*) and cytotoxicity of (*R*)-(-)-**4** and (*S*)-(+)-**4**.

				IC_{50} (μM)[a]								CC_{50}[b] (μM)
CPD	R	R_1	R_2	Tb[c]	SI[d]	Tc[e]	SI[f]	Ld[g]	SI[h]	Pf[i]	SI[j]	
(*S*)-(+)-**4**	Cl	H	2,4-Cl_2	12.19	-	0.017	327	5.02	1	0.11	51	5.56
(*R*)-(-)-**4**	Cl	H	2,4-Cl_2	9.21	-	0.0009	2844	3.77	-	0.092	28	2.56
(±)-**4**	Cl	H	2,4-Cl_2	17.33	-	0.035	275	3.77	3	0.16	60	9.61

[a]Concentration of compound required to decrease parasite viability by 50% compared to the number of parasites grown in the absence of the test compound [b]Cytotoxicity measurement for L6 cells; [c]*Trypanosoma brucei rhodesiense*, STIB900 trypomastigote; [d]Calculated as (CC_{50})/(IC_{50} for *T.b. rhodesiense*); [e]*Trypanosoma cruzi*, Tulahuen C2C4 amastigote; [f]Calculated as (CC_{50})/(IC_{50} for *T. cruzi*); [g]*Leishmania donovani,* MHOM/ET/67/L82 axenic amastigote; [h]Calculated as (CC_{50})/(IC_{50} for *L. donovani*); [i]*Plasmodium falciparum* K1 erythrocytic stage; [j]Calculated as (CC_{50})/(IC_{50} for *P. falciparum*).

Target-based studies. Binding affinity of five compounds was assessed in the 96-well format, where four of the five derivatives (**5i, 6b, 6c** and **8b**) saturated 5 μM TcCYP51 at equimolar concentrations; no further changes occurred upon doubling compound concentration (Figure 6). All five compounds bound to TcCYP51 produced type II low-spin difference spectra with a trough at 388 nm and a peak at 426 nm (Figure 6), indicative of heterocycle coordination to the heme iron.[49] Notably, compound **4** and analogues were recently proven to have a similar behavior, showing

high affinity towards TcCYP51 within the nanomolar range.[34] Differently, one compound, **6a**, did not reach saturation even at 10 μM, suggesting lower binding affinity. To determine dissociation constant, K_D, spectral titration of 2 μM TcCYP51 with **6a** was performed manually in 1-cm split chamber tandem spectrophotometer cuvette (Figure 7). The dissociation constant of 5.5±1.6 μM was extrapolated from the binding isotherm (Figure 7, Inset) using the quadratic Morrison equation. The dissociation constants could not be calculated for the tighter binding compounds due to enzyme saturation reached after the addition of a molar equivalent of the inhibitor to 2 μM TcCYP51. When sub-stoichiometric concentrations of compounds were titrated into the enzyme solution, a linear increase in signal was observed up until the equivalence point, after which no further increase in signal was detected.

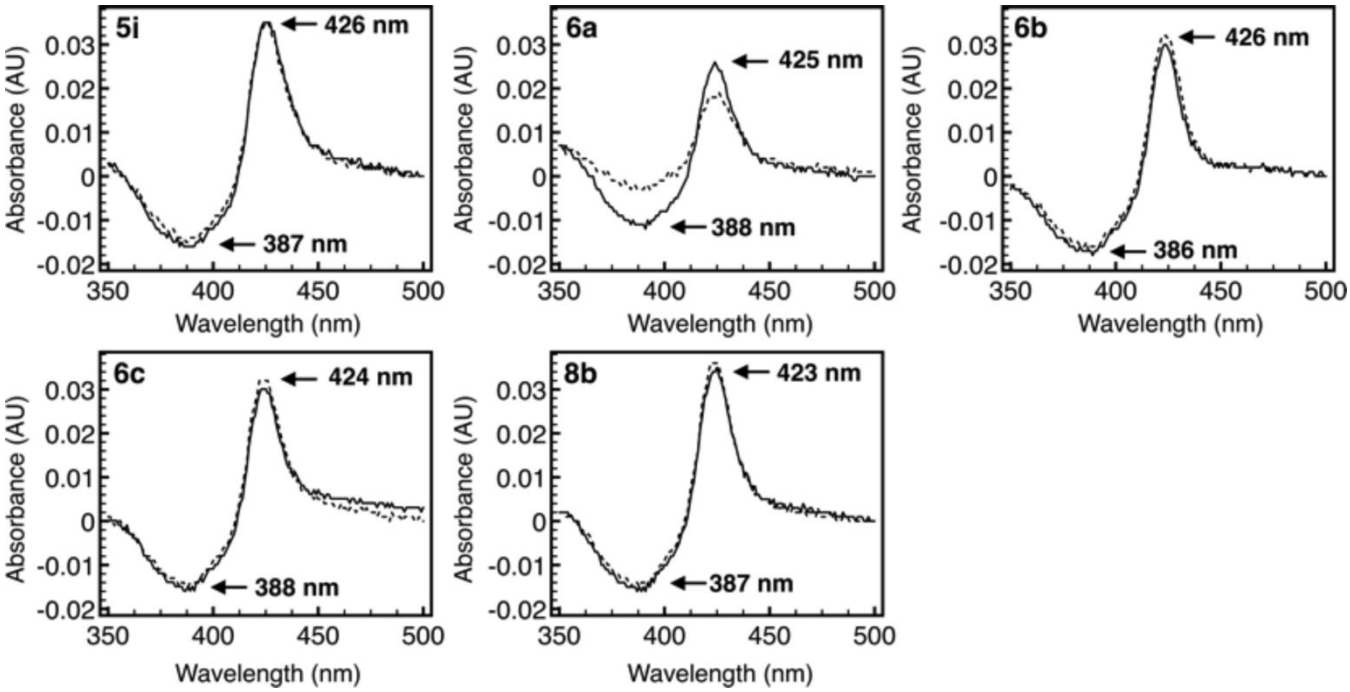

Figure 6. UV-vis binding assay in 96-well format shows overlap of the difference spectra at 5 μM (dashed line) and 10 μM (solid line) for **5i**, **6b**, **6c** and **8b**, indicating target saturation at 1:1 molar enzyme: inhibitor ratio. TcCYP51 concentration was 5 μM.

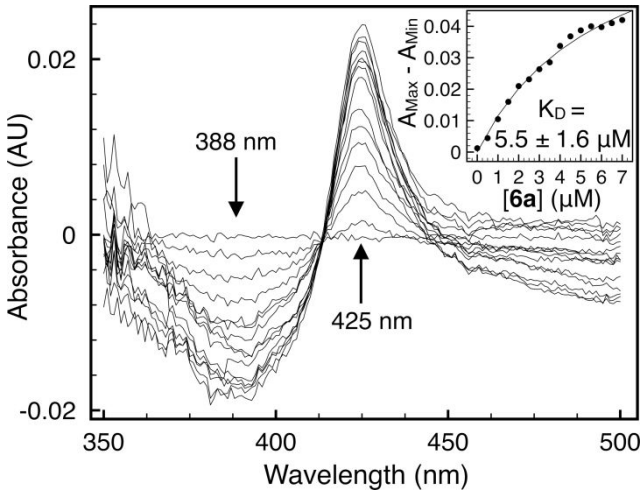

Figure 7. UV-vis spectral analysis of TcCYP51-**6a** interactions in 1-cm quartz cuvette. Type II UV-vis difference spectra resulted from adding **6a** in 500 nM increments to 2 μM TcCYP51. Inset: binding isotherm for **6a** was generated by plotting the differences between the absorbance minimum at 388 nm and the absorbance maximum at 425 nm as a function of drug concentration.

Inhibition of human CYPs *in vitro*. Five compounds have been selected and assayed against relevant CYP enzymes *in vitro* to evaluate cross-reactivity of these azole

compounds with human drug-metabolizing proteins. In particular, derivatives endowed with the most promising *in vitro* nanomolar potencies against *T. cruzi* (**6a-c**, **8b**) and the reference compound **4** were tested against cytochromes P450 CYP3A4, CYP1A2 and CYP2D6, representing the major human CYPs involved in the oxidative metabolism of vast majority of drugs in clinical use and drug-drug interactions.[27,30] The rate of metabolite formation of CYP450-specific probes (See Table S5 Supporting Information) by CYP3A4, CYP1A2, CYP2D6 and enzymes was measured in the presence and absence of increasing concentrations of **4**, **6a-c** and **8b**. Results of the inhibitory potential of our azole compounds toward this panel of CYPs are reported in Table 3 and expressed as IC_{50}, in comparison with the inhibitory potencies of prototypical CYP inhibitors (ketoconazole for CYP3A4; furafylline for CYP1A2; quinidine for CYP2D6).

Compounds inhibited all CYP450 enzymes in the low micromolar range, with the exception of **8b** that showed $IC_{50} > 30$ μM for CYP1A2. **6a-c**, **8b** proved to be the weakest CYP2D6 inhibitors resulting from 200 to 600 times less active in respect of the potent 2D6 inhibitor quinidine.

Differently, although CYP3A4 was inhibited to a higher extent by tested azole compounds, all derivatives proved to be less effective in inhibiting the enzyme in respect of ketoconazole. The most promising results were highlighted by compounds

6a,**b** which showed a 3-4 times lower interfering activity in respect of the reference 3A4 inhibitor.

Regarding the interference with CYP1A2, despite derivatives **6a-c** proved to affect the enzymatic activity at submicromolar-micromolar concentrations, it is worthy to note that the reference compound **4** displayed a 3 times lower inhibition in respect of the reference 1A2 inhibitor furafylline. Noteworthy, the new derivative **8b** did not inhibit such enzyme even at the high concentration employed in the assay (IC_{50} > 30 μM).

Overall, concerning their potencies against human CYPs, derivatives **4**, **8b** and **6b** resulted the less interfering and thus, the most encouraging compounds. In particular, the first two proved to be less potent than the respective reference inhibitors against each human CYP enzymes, while derivative **6b**, despite showing IC_{50} comparable with furafylline against CYP1A2, inhibited all the three CYP enzymes only at micromolar concentrations. The importance of this data is further strengthen by the proven *in vivo* efficacy of this compound in mice model (see following paragraph).

It is worthy to note that the inhibitory potencies against human CYPs ranged between the micromolar and submicromolar range, whereas all of these compounds proved to inhibit *T. cruzi* growth from one to three order of magnitude lower concentrations in *in vitro* assays.

Moreover, except of compound **6a** and similarly to the previously reported analogues[34], all derivatives displayed very high affinities against TcCYP51 estimated in the nanomolar range, that, notably, correlate with the anti-*T. cruzi* inhibitory potencies.

Taken together, these biological results indicate that our azole compounds show higher affinity towards TcCYP51 in respect of human CYPs, proving to inhibit parasite enzyme and growth at much lower concentrations in respect of the ones useful to disrupt human metabolic enzymes. According to this, it can be stated that negligible interference on human enzymes is expected at the very low concentrations required to exert antiprotozoal effects.

Finally, although cross-reactivity with human CYPs need further optimization, these preliminary data highlighted promising results indicating that there is still room for further improvement of selectivity for such antiprotozoal agents.

Table 3. Enzymatic inhibition of human CYPs *in vitro*.

	IC$_{50}$ (μM)[a]		
CPD	CYP3A4	CYP1A2	CYP2D6
6a	1.4	0.4	4.0
6b	1.1	2.0	
6c	0.9	1.2	3.0
8b	0.9	>30	
4	0.8	7.0	2.0
KET[b]	0.4	2.3	6.0
FUR[c]			1.3
QUI[d]			0.01

[a]Concentration of compound required to decrease enzymatic activity by 50%;[b]ketoconazole; [c]furafylline; [d]quinidine.

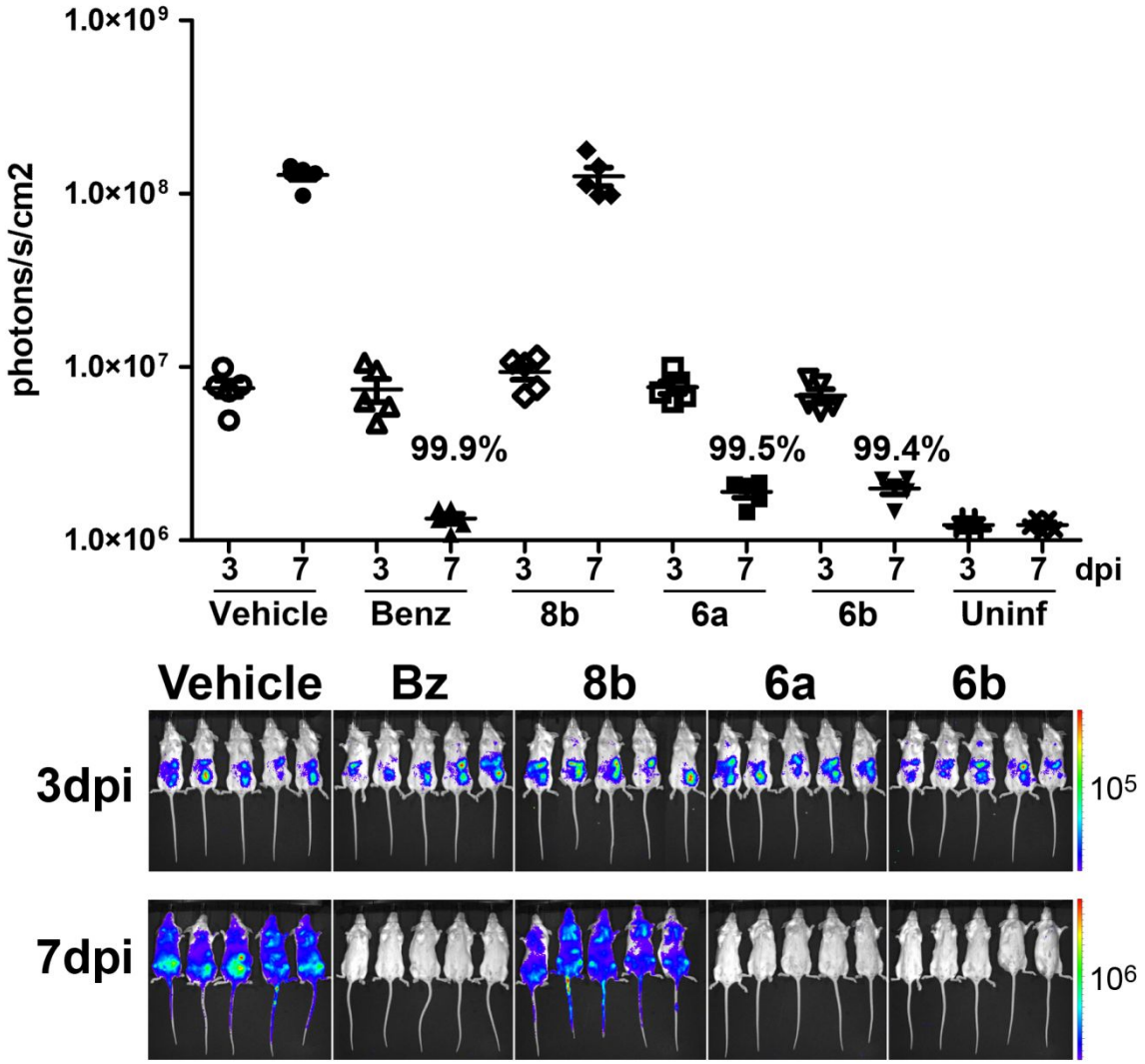

Figure 8. Luminescence in *T. cruzi*-infected mice measured upon luciferin injection 3 days post-infection (dpi) prior to treatment and 7 dpi after four days of treatment. Bz was used as reference drug. Bz, **6a** and **6b** significantly inhibited *T. cruzi* parasitemia, 99.9%, 99.5% and 99.4%, respectively; values significantly different from vehicle-treated controls ($p \leq 0.05$ in Student t-test). **8b** showed no *in vivo* activity.

***In vivo* studies. 6a, 6b** and **8b**, that were three of the most potent compounds found active *in vitro* against *T. cruzi* were assessed in mice infected with *T. cruzi* expressing the luciferase marker. The

treatment begun 3 days post-infection (dpi) and compounds were administered at 25 mg/kg, i.p., b.i.d. for 4 consecutive days. General animal health was monitored daily. No adverse clinical symptoms indicative of toxicity (hunched posture, lack or grooming, reduced mobility, loss of weight) were observed during the experiment. Mice were imaged at 7 dpi, bioluminescence was quantified and plotted for each group of five animals as indicated in Figure 8. The treatment with **6a** and **6b** reduced parasitemia by 99.5% and 99.4%, respectively, while the reference drug, Bz, administered at 50 mg/kg, induced 99.9% of inhibition (Figure 8). On the other hand, treatment with compound **8b** did not affect parasitemia in mice, despite that **8b** displayed 5 nM IC_{50} against *T. cruzi* in cell-based assay. The lack of *in vivo* activity indicates low bioavailability of **8b**.

CONCLUSIONS

In this paper we described the design, synthesis and biological evaluation as antiprotozoal agents of novel imidazole-based derivatives **5a-l**, **6a-c**, **7a-f** and **8a-c** that were designed starting from the hit compounds recently reported by our group.[34] The most potent newly synthesized analogs displayed double-digit micromolar activity against *T. brucei,* single-digit micromolar activity against *L. donovani* and range of nanomolar activities against *P. falciparum* and *T. cruzi* (Table 1). Some of the new compounds proved to be endowed with improved anti-*T. cruzi* and antiplasmodial activities compared to their analogs previously reported by us.[34] Although none of new derivatives resulted more potent than ART, compound **5h** displayed the best antiplasmodial activity proving to be 3 times more potent than the reference drug CHQ with high selectivity index (SI = 253).

Derivatives **5i**, **6a-c** and **8b** displayed anti-*T. cruzi* activities in the low nanomolar range and are endowed with high selectivity indices (373 < SI < 4030). The role of stereochemistry in the inhibitory activity, was assessed by enantiomeric separation of a racemic mixture of **4**. In fact, the enantiomer (*R*)-(-)-**4** had the highest anti-*T. cruzi* activity (eutomer), with IC_{50} of 0.9 nM. Effective binding of these azoles to recombinant *T. cruzi* CYP51 suggests that this enzyme may be targeted within *T. cruzi* parasite, although **6a** shows a lower affinity if compared to the remaining tested compounds.

Preliminary evaluation of selectivity towards relevant drug-metabolizing enzymes showed promising results, although cross-reactivity with human CYPs require further optimization for such antiprotozoal agents.

Very interstingly, **6a** and **6b** displayed remarkable efficacy in the 4-day animal model of infection resulting in >99% reduction of *T. cruzi* parasitemia in mice, with no acute toxicity observed in this animal model. Notably, compound **8b** was inactive in *in vivo* assays, suggesting that it is endowed with low bioavailability. Conversely, a comparison between the activities of **6a** and **6b** suggests that, both compounds are potent and bioavailable anti-*T. cruzi* agents, but while **6b** is probably targeting CYP51, **6a** could act via a yet unknown target. A different possibility is that **6a** has a so high bioavailability that can overcome its low potency against the CYP51 target.

EXPERIMENTAL SECTION

Chemistry. *General.* Reagents were purchased from Sigma-Aldrich and were used as received. Reaction progress was monitored by TLC using Merck silica gel 60 F_{254} (0.04-0.063 mm) with detection by UV (214 or 254 nm). Merck silica gel 60 or aluminum oxide 90 (active neutral) were used for column chromatography. Melting points (uncorrected) were determined in open Pyrex capillary tubes using a Buchi 510 melting point apparatus. Compounds purity were always > 95% determined by combustion analysis. Analytical results agreed to within ± 0.40% of the theoretical values. Nuclear Magnetic Resonance Spectroscopy (^{1}H NMR) were obtained using a Bruker Avance system, operating at 400 MHz. Concentration of solution after reactions and extractions involved the use of a rotary evaporator operating at reduced pressure of approximately 20 Torr. Dimethylsulfoxide-d_6 99.9% (code 44,139-2), deuterochloroform 98.8% (code 41,675-4) and acetone-d_6 99.9% (code 44,486-3) of isotopic purity (Aldrich) were used. Solvents were reagent grade and, when necessary, were purified and dried by standard methods. Organic solutions were dried over anhydrous sodium sulfate (Merck).

Microwave irradiation experiments. Microwave reactions were conducted using a CEM Discover system unit (CEM. Corp. Matthews, NC). The machine consists of a continuous focused microwave-power delivery system with operator selectable power output from 0 to 300 W. The temperature of the contents of the vessel was monitored using a calibrated infrared temperature control mounted under the reaction vessel. All experiments were performed using a stirring option whereby the contents of the vessel are stirred by means of a rotating magnetic plate located below the floor of the microwave cavity and a Teflon-coated magnetic stir bar in the vessel.

Chemical, physical, analytical and spectroscopic data for derivatives **5a-k**, **6a-c, 7a-f** and **8a-c** are as follows**.** 4-Methylbenzaldehyde (**9a**), 4-ethylbenzaldehyde (**9b**), 4-isopropylbenzaldehyde (**9c**), 4-methoxybenzaldehyde (**9d**), 2-naphthaldehyde (**9h**) are commercially available. Syntheses and characterization of compounds 4-chloro-2-(1*H*-pyrrol-1-yl)benzaldehyde (**9e**), 5-chloro-[1,1'-biphenyl]-2-carbaldehyde (**9g**), 4-chloro-1-naphthaldehyde (**9i**) are described in literature [35-37]. A mixture of aldehydes **9f** and **9j** (4:1 ratio) was employed for the synthesis of the chalcone **10f.** For chemical, physical, analytical and spectroscopic data of intermediates **9f,j,k, 10b,c,e-j**, **11a-j**, **12a-j, 15b,c**, **16a-c**, **19a-c**, **20a-f**, **21a-c**, **22a-f**, see Supporting Information. Chemical and physical data for derivatives **13, 14** and **17** are as follows. Spectroscopic data for intermediate **14** are in Supporting Information, while for **13** and **17** are previously reported[40]. Syntheses and characterization of compounds **10a,d, 18a-e** are described in literature.[38,39,41-43]

General procedure A (GP-A) to obtain Imidazoles 5a-j, 6a-c, 7a-f and **8a-c.** 1,1'-Carbonyldiimidazole (19.3 mmol) was added portionwise to a solution of the proper carbinol **12a-j, 16a-c, 21a-c** and **22a-f** (4.8 mmol) in anhydrous acetonitrile (100mL). The reaction mixture was stirred at room temperature for the proper time. The solvent was removed and the residue was dissolved in ethyl acetate. The organic solution was washed with brine and dried over anhydrous Na_2SO_4. Removal of the solvent afforded crude imidazole derivatives **5a-j, 6a-c, 7a-f** and **8a-c**, which were purified by column chromatography using aluminum oxide as stationary phase.

For each compound yield (%), melting point (°C), recrystallization solvent, reaction time, eluent, IR spectra, ^{1}H-NMR and elemental analysis are reported.

General procedure B (GP-B) to obtain Chalcones 10a-j. A solution of the appropriate benzaldehyde **9a-e,i** or a mixture of isomers **9f** and **9j,** (26.5 mmol) and 2',4'-dichloroacetophenone (or 4'-dichloroacetophenone for derivative **10h**) (26.5 mmol) in 65 mL of ethanol was added to a solution of NaOH (65 mmol) in 55 mL of H_2O was added. The mixture was stirred at room temperature for 15 h. The ethanol was removed at reduced pressure and the reaction mixture was neutralized with acetic acid and extracted with ethyl acetate. The combined organic phases were washed with 1 N HCl, brine, dried over Na_2SO_4 and evaporated at reduced pressure to obtain pure compounds **10a-d,i** or crude products **10e-h** that were purified by column chromatography using aluminum oxide as stationary phase. For each compound yield (%), melting point (°C), recrystallization solvent, eluent, IR spectra, ^{1}H-NMR and elemental analysis are reported in Supporting Information.

General procedure C (GP-C) to obtain Pyrroles 11a-j. To a suspension of NaH 60% (55 mmol) in 55 mL of anhydrous diethyl ether under argon stream was added dropwise a solution of **10a-j** (25 mmol) and TosMIC (25 mmol) in diethyl ether/DMSO 2:1 (165 mL) at room temperature. After the addition, the reaction mixture was stirred at room temperature for the proper time.

For derivative **11c,** the reaction was diluted with water and the solid that formed was filtered, washed with water, petroleum ether to give the pure product **11c** as solid.

For derivatives **11a,b,d-j,** the mixture was diluted with water and extracted with ethyl acetate. The combined organic phases were washed with brine, dried over Na_2SO_4 and evaporated at reduced pressure. The crude products were purified by column chromatography (aluminum oxide/ chloroform) to furnish the pure derivatives **11a,b,d-j**. For each compound yield (%), melting point (°C), recrystallization solvent, reaction time, IR spectra, ^{1}H-NMR and elemental analysis are reported in Supporting Information.

General procedure D (GP-D) to obtain Carbinoles 12a-j. A solution of the proper ketones **11a-j** (4.4 mmol) in THF anhydrous (55 mL) was added dropwise to a suspension of $LiAlH_4$ (6.6 mmol) in the same solvent (30 mL) cooled at 0 °C under argon atmosphere.

For derivatives **12a-f,i** an additional amount of of $LiAlH_4$ (6.6 mmol) was added after 1h and the mixture was stirred at room temperature for the proper time, while for derivatives **12g,h,j** complete reduction was achieved after 30-45 min without further reactant additions.

The mixture was carefully treated with crushed ice/water and the inorganic precipitate that formed was removed. The solution was concentrated at reduced pressure and extract with chloroform. The organic solution was washed with brine, dried and evaporated. Crude carbinols **12a-j** were used for the next reaction without further purification. For each compound yield (%), melting point (°C), recrystallization solvent, reaction time, IR spectra, are reported in Supporting Information.

General procedure E (GP-E) to obtain *N*-alkyl pyrroles 15b,c. The proper alkyl halide (25 mmol; iodomethane for derivative **15b** and allyl bromide for derivative **15c**) was added to a suspension of **14** (3.16 mmol) and potassium carbonate anhydrous (6.3 mmol) in DMF (5.2 mL) and the reaction was stirred at 90°C for 3.5 h.

For derivative **15b**, the mixture was diluted with water and extracted with ethyl acetate. The organic layer was washed with brine, dried over anhydrous Na_2SO_4, filtered, and evaporated in vacuum to achieve crude **15b**.

For derivative **15c**, additional amounts of allyl bromide (12.64 mmol) and potassium carbonate (3.16 mmol) were added after 3.5 h and the mixture was stirred at 90°C for 2.5 hours and then at room temperature for 2 days. The reaction was diluted with water and extracted with ethyl acetate. The organic phase was washed with brine, dried and the solvent was evaporated under reduced pressure to obtain crude **15c**.

Crude products **15b,c** were purified on column chromatography using alumina as stationary phase and chloroform as eluent yielding pure derivatives **15b,c**.

For each compound yield (%), melting point (°C), recrystallization solvent, IR spectra, ^{1}H-NMR and elemental analysis are reported in Supporting Information.

General procedure F (GP-F) to obtain Alcohols 16a-c, 21a-c and 22a-f. $NaBH_4$ (13 mmol) was added to a well-stirred solution of the appropriate ketones **14, 15b,c**, **19a-c** or **20a-f** (2.6 mmol) in 17 mL of anhydrous THF and the mixture was stirred at room temperature and/or reflux for the proper time. Additional amounts of sodium borohydride were added for the syntheses of derivatives **21a,b, 22a,d,e.**

The reaction was treated with water and the mixture was concentrated at reduced pressure and extract with ethyl acetate. The organic solution was washed with brine, dried and evaporated. Crude carbinols **16a-c, 21a-c** and **22a-f** were used for the next reaction without further purification.

For each compound yield (%), melting point (°C), recrystallization solvent, reaction time and temperature, additional amounts of sodium borohydride (if necessary), IR spectra are reported in Supporting Information.

General procedure G (GP-G) to obtain Ketones 19a-c and 20a-f. A solution of the proper benzoyl chloride (121 mmol) in DCM (107 mL) was added to a suspension of aluminium trichloride (121 mmol) in the same solvent (107 mL). The clear solution was slowly dropped into a well-stirred solution of the appropriate pyrrole (56.3 mmol) in 26 mL of DCM. The reaction was stirred at room temperature overnight and then poured into crushed ice (300 g) and acidified by adding concentrated HCl (16 mL). The organic layer was separated and the aqueous phase was extract with chloroform. The extracts were collected, washed with brine and Na_2CO_3 saturated solution, brine again and dried over anhydrous Na_2SO_4. After evaporation of the solvent, the residue was purified by column chromatography using aluminum oxide as stationary phase to furnish pure derivatives **19a-c** and **20a-f**.

For each compound yield (%), melting point (°C), recrystallization solvent, chromatographic system, IR spectra, ^{1}H-NMR and elemental analysis are reported in Supporting Information.

1-[(2,4-Dichlorophenyl)[4-(*p*-tolyl)-1*H*-pyrrol-3-yl]methyl]-1*H*-imidazole (5a). Compound **5a** was prepared from **12a** by means of GP-A**.** 55% as orange solid; 197-200 °C; ethanol/petroleum ether; 15 h; ethyl acetate; IR ν 3120 (NH) cm^{-1}. ^1H NMR ($CDCl_3$) δ 2.38 (s, 3H, CH_3), 6.33 (s, 1H, pyrrole C5-H), 6.80 (s, 1H, imidazole H), 6.84 (d, 1H benzene H), 6.91-6.94 (m, 2H, pyrrole C2-H and CH), 7.04 (d, 2H, benzene H), 7.13-7.14 (m, 3H, imidazole H and benzene H), 7.23 (d, 1H, benzene H), 7.43 (d, 1H, benzene H), 7.54 (s, 1H, imidazole H), 9.07 (br s, 1H, NH). Anal. Calcd for $C_{21}H_{17}Cl_2N_3$: C, 65.98; H, 4.48; N, 10.99; Cl, 18.55 %. Found C, 66.06; H, 4.49; N, 11.03; Cl, 18.57%.

1-[(2,4-Dichlorophenyl)[4-(4-ethylphenyl)-1*H*-pyrrol-3-yl]methyl]-1*H*-imidazole (5b). Compound **5b** was prepared from **12b** by means of GP-A**.** 49% as yellow solid; 194-197 °C; toluene/cyclohexane; 15 h; ethyl acetate IR ν 3126 (NH) cm^{-1}. ^1H NMR ($CDCl_3$) δ 1.28 (q, 3H, $CH_2\mathit{CH_3}$), 2.69 (t, 2H, $\mathit{CH_2}CH_3$), 6.33 (s, 1H, pyrrole C5-H), 6.80 (s, 1H, imidazole H), 6.84 (d, 1H benzene H), 6.92 (s, 1H, CH), 6.94 (t, 1H, pyrrole C2-H), 7.06 (d, 2H, benzene H), 7.14-7.18 (m, 3H, benzene H and imidazole H), 2.24 (dd, 1H, benzene H), 7.43 (d, 2H, benzene H), 7.51 (s, 1H, imidazole H), 8.65 (br s, 1H, NH). Anal. Calcd for $C_{22}H_{19}Cl_2N_3$: C, 66.67; H, 4.83; N, 10.60; Cl, 17.89 %. Found C, 66.56; H, 4.82; N, 10.56; Cl, 17.86%.

1-[(2,4-Dichlorophenyl)[4-(4-isopropylphenyl)-1*H*-pyrrol-3-yl]methyl]-1*H*-imidazole (5c). Compound **5c** was prepared from **12c** by means of GP-A**.** 41% as yellow solid; 205-208 °C; toluene/cyclohexane; 15 h; ethyl acetate; IR ν 3126 (NH) cm^{-1}. ^1H NMR ($CDCl_3$) δ 1.30 (d, 6H, $CH\mathit{(CH_3)_2}$), 2.93 (m, 1H, $\mathit{CH}(CH_3)_2$), 6.33 (s, 1H, pyrrole C5-H), 6.81 (s, 1H, imidazole H), 6.84 (d, 1H benzene H), 6.92 (s, 1H, CH), 6.85 (t, 1H, pyrrole C2-H), 7.06 (d, 2H, benzene H), 7.14 (s, 1H, imidazole H), 7.19 (d, 2H, benzene H), 2.23 (dd, 1H, benzene H), 7.43 (d, 2H, benzene H), 7.51 (s, 1H, imidazole H), 8.74 (br s, 1H, NH). Anal. Calcd for $C_{23}H_{21}Cl_2N_3$: C, 67.32; H, 5.16; N, 10.24; Cl, 17.28 %. Found C, 67.40; H, 5.17; N, 10.25; Cl, 17.30%.

1-[(2,4-Dichlorophenyl)[4-(4-methoxyphenyl)-1*H*-pyrrol-3-yl]methyl]-1*H*-imidazole (5d). Compound **5d** was prepared from **12d** by means of GP-A**.** 51% as brown solid; 183-185 °C; ethanol;

100 min; ethyl acetate; IR ν 3124 (NH) cm^{-1}. ^1H NMR ($CDCl_3$) δ 3.82 (s, 3H, CH_3), 6.32 (s, 1H, pyrrole C5-H), 6.77-6.91 (m, 6H, benzene H, pyrrole C2-H, CH and imidazole H), 7.02 (d, 2H, benzene H), 7.15 (s, 1H, imidazole H), 7.22 (d, 1H, benzene H), 7.44 (d, 1H, benzene H), 7.56 (s, 1H, imidazole H), 8.80 (br s, 1H, NH). Anal. Calcd for $C_{21}H_{17}Cl_2N_3O$: C, 63.33; H, 4.30; N, 10.55; Cl, 17.80 %. Found C, 63.46; H, 4.31; N, 10.56; Cl, 17.85%.

1-[[4-[4-Chloro-2-(1*H*-pyrrol-1-yl)phenyl]-1*H*-pyrrol-3-yl](2,4-dichlorophenyl)methyl]-1*H*-imidazole (5e). Compound **5e** was prepared from **12e** by means of GP-A**.** 24 % as yellow solid; 158-160 °C; *n*-hexane; 15 h; *n*-hexane: ethyl acetate 5:2; IR ν 3331 (NH) cm^{-1}. ^1H NMR (DMSO-d_6) δ 5.44 (s, 1H, pyrrole C5-H), 6.15-6.21 (m, 3H, imidazole H and pyrrole β-proton), 6.82 (t, 1H, pyrrole C2-H), 6.94 (s, 1H, CH), 7.03-7.20 (m, 6H, pyrrole α-proton and benzene H), 7.37 (s, 1H, imidazole H), 7.44 (d, 2H, benzene H), 7.55 (s, 1H, imidazole H), 11.14 (br s, 1H, NH). Anal. Calcd for $C_{24}H_{17}Cl_3N_4$: C, 61.62; H, 3.66; N, 11.98; Cl, 22.74 %. Found C, 61.52; H, 3.65; N, 12.01; Cl, 22.69%.

1-[[4-[4-Chloro-2-(thiophen-2-yl)phenyl]-1*H*-pyrrol-3-yl](2,4-dichlorophenyl)methyl]-1*H*-imidazole (5f). Compound **5f** was prepared from **12f** by means of GP-A**.** 95 % as brown oil; 15 h ; ethyl acetate; IR ν 3303 (NH) cm^{-1}. ^1H NMR (Acetone-d_6) δ 6.11 (s, 1H, CH), 6.15 (m, 1H, pyrrole H), 6.53 (m, 1H, pyrrole H), 6.59-6.62 (m, 2H, imidazole H and benzene H), 6.69 (d, 1H, benzene H), 6.79-6.85 (m, 2H, imidazole H and tiophene β-proton), 6.93-6.97 (m, 2H, benzene H and tiophene β-proton), 7.06-7.11 (m, 2H, benzene H), 7.19 (d, 1H imidazole H), 7.26 (dd, 1H, tiophene α-proton), 7.32 (d, 1H, benzene H), 10.2 (br s, 1H, NH). Anal. Calcd for $C_{24}H_{16}Cl_3N_3S$: C, 59.46; H, 3.33; N, 8.67; Cl, 21.94; S, 6.61%. Found C, 59.50; H, 3.32; N, 8.66; Cl, 21.90; S, 6.60%.

1-[[4-(5-Chloro-[1,1'-biphenyl]-2-yl)-1*H*-pyrrol-3-yl](2,4-dichlorophenyl)methyl]-1*H*-imidazole (5g). Compound **5g** was prepared from **12g** by means of GP-A**.** 100% as yellow solid; 250 °C; toluene; 20h; ethyl acetate; IR ν 3100 (NH) cm^{-1}. ^1H NMR (DMSO-d_6) δ 6.19-6.22 (s, 1H, pyrrole C5-H and CH), 6.62-7.71 (m, 15H, imidazole H, pyrrole C2-H and benzene H), 10.95 (s, 1H, NH). Anal. Calcd for $C_{26}H_{18}Cl_3N_3$: C, 65.22; H, 3.79; N, 8.78; Cl, 22.21 %. Found C, 65.19; H, 3.78; N, 8.77; Cl, 22.19%.

1-[[4-(5-chloro-[1,1'-biphenyl]-2-yl)-1*H*-pyrrol-3-yl](4-chlorophenyl)methyl]-1*H*-imidazole (5h). Compound **5h** was prepared from **12h** by means of GP-A**.** 77% as yellow solid; 79-80 °C; toluene 15 h; ethyl acetate; IR ν 3413 (NH) cm^{-1}. ^1H NMR ($CDCl_3$) δ 5.53 (s, 1H, CH), 6.09 (m, 1H, pyrrole C5-H), 6.51-6.53 (m, 3H, benzene H and imidazole H), 6.76 (t, 1H, pyrrole C2-H), 6.93 (t, 1H, imidazole), 7.1 (d, 1H, benzene H), 7.14-7.19 (m, 5H, benzene H), 7.29-7.38 (m, 4H, benzene H),7.76 (s, 1H, imidazole H), 8.40 (br s, 1H, NH). Anal. Calcd for $C_{26}H_{19}Cl_2N_3$: C, 70.28; H, 4.31; N, 9.46; Cl, 15.96 %. Found C, 70.32; H, 4.30; N, 9.47; Cl, 15.94%.

1-[(2,4-Dichlorophenyl)[4-(naphthalen-2-yl)-1*H*-pyrrol-3-yl]methyl]-1*H*-imidazole (5i). Compound **5i** was prepared from **12i** by means of GP-A**.** 77% as brown oil; 45 min; ethyl acetate; IR ν 3303 (NH) cm^{-1}. ^1H NMR ($CDCl_3$) δ 6.36 (s, 1H, pyrrole C5-H), 6.84 (s, 1H, imidazole H), 6.95 (s, 1H, CH), 7.04 (t, 1H, imidazole H), 7.16-7.21 (m, 2H, benzene H and pyrrole C2-H), 7.26-7.46 (m, 5H, benzene H, imidazole H and naphthalene H), 7.55 (m, 2H, naphthalene H), 7.68 (m, 1H, naphthalene H), 7.80 (m, 2H, naphthalene H), 8.90 (br s, 1H, NH). Anal. Calcd for $C_{24}H_{17}Cl_2N_3$: C, 68.91; H, 4.10; N, 10.05; Cl, 16.95 %. Found C, 68.92; H, 4.11; N, 10.01; Cl, 16.89%.

1-[[4-(4-Chloronaphthalen-1-yl)-1*H*-pyrrol-3-yl](2,4-dichlorophenyl)methyl]-1*H*-imidazole (5j). Compound **5j** was prepared from **12j** by means of GP-A**.** 49% as brown solid; 197-200 °C; *n*-hexane; 15 h; ethyl acetate: ethanol 10:0.5; IR ν 3310 (NH) cm^{-1}. ^1H NMR ($CDCl_3$) δ 6.42-6.46 (m, 2H, CH and pyrrole C5-H), 6.72-6.74 (m, 2H, benzene H and imidazole H), 6.90-6.99 (m, 3H, imidazole H, pyrrole C2-H and naphthalene H), 7.12 (dd, 1H, benzene H), 7.32-7.47 (m, 4H, benzene H, imidazole H and naphthalene H), 7.58 (m, 1H, naphthalene H), 7.86 (m, 1H, naphthalene H), 8.29 (m, 1H, naphthalene H), 9.29 (br s, 1H, NH). Anal. Calcd for $C_{24}H_{16}Cl_3N_3$: C, 63.67; H, 3.56; N, 9.28; Cl, 23.49 %. Found C, 63.62; H, 3.55; N, 9.29; Cl, 23.51%.

Synthesis of 1-[(2,4-dichlorophenyl)[4-[4-(methylsulfonyl)phenyl]-1*H*-pyrrol-3-yl]methyl]-1*H*-imidazole (5k). To a cooled solution of **5l** (1.12 mmol) in methanol (32 mL) was added a solution of oxone (1.82 mmol) in water (8 mL) and the mixture was stirred at room temperature for 18 h. The

reaction was poured into water, concentrated at reduced pressure, extract with ethyl acetate. The combined organic phases were washed with brine, dried over Na_2SO_4 anhydrous, concentrated at reduced pressure afforded pure imidazole **5k** as yellow solid (quantitative yield). 201-203 °C, *i*PrOH; IR ν 3131 (NH), 1301 and 1147 (SO_2) cm^{-1}. ^1H NMR ($CDCl_3$) δ 3.11 (s, 3H, CH_3), 6.43 (s, 1H, pyrrole C5-H), 6.85 (d, 1H, benzene H), 6.90 (s, 1H, imidazole H), 6.99 (s, 1H, pyrrole C2-H), 7.12 (s, 1H, CH), 7.24-7.37 (m, 4H, benzene H and imidazole H), 7.49 (d, 1H, benzene H), 7.77 (s, 1H, imidazole H), 7.90 (d, 2H, benzene H), 9.37 (br s, 1H, NH). Anal. Calcd for $C_{21}H_{17}Cl_2N_3O_2S$: C, 56.51; H, 3.84; N, 9.41; Cl, 15.89; S, 7.18%. Found C, 56.70; H, 3.83; N, 9.40; Cl, 15.87; S, 7.19%.

1-[(4-Chlorophenyl)[5-(4-chlorophenyl)-1*H*-pyrrol-3-yl]methyl]-1*H*-imidazole (6a). Compound **6a** was prepared from **16a** by means of GP-A**.** 67% as yellow solid; 289-291 °C; toluene; 80 min; ethyl acetate:methanol 5:1; IR ν 3113 (NH) cm^{-1}. ^1H NMR (DMSO-d_6) δ 6.44 (s, 1H, pyrrole H), 6.46 (s, 1H, CH), 6.57 (s, 1H, pyrrole H), 6.63 (d, 1H, J_o = 8 Hz, imidazole H), 6.84 (d, 1H, J_o = 8 Hz, imidazole H), 7.11 (d, 2H, J_o = 8.8 Hz benzene H), 7.29-7.35 (m, 4H, benzene H), 7.53 (d, 2H, J_o = 8.8 Hz benzene H), 7.62 (s, 1H, imidazole H), 8.52 (s, 1H, NH pyrrole). Anal. Calcd for $C_{20}H_{15}Cl_2N_3$: C, 65.23; H, 4.11; N, 11.41; Cl, 19.25%. Found C, 65.20; H, 4.12; N, 11.43; Cl, 19.27%.

1-[(4-Chlorophenyl)[5-(4-chlorophenyl)-1-methyl-1*H*-pyrrol-3-yl]methyl]-1*H*-imidazole (6b). Compound **6b** was prepared from **16a** by means of GP-A**.** 72% as yellow oil; 100 min; chloroform; ^1H NMR (DMSO-d_6) δ 3.53 (s, 3H, CH_3), 5.97 (s, 1H, pyrrole

H), 6.42 (s, 1H, pyrrole H), 6.49 (s, 1H, CH), 7.01-7.07 (m, 3H, imidazole H and benzene H), 7.19-7.33 (m, 7H, imidazole H and benzene H), 8.32 (s, 1H, imidazole H). Anal. Calcd for $C_{21}H_{17}Cl_2N_3$: C, 65.98; H, 4.48; N, 10.99; Cl, 18.55%. Found C, 65.93; H, 4.49; N, 11.02; Cl, 18.57%.

1-[[1-Allyl-5-(4-chlorophenyl)-1*H*-pyrrol-3-yl](4-chlorophenyl)methyl]-1*H*-imidazole (6c). Compound **6c** was prepared from **16a** by means of GP-A. 82% as brown oil; 15h; chloroform; ^{1}H NMR (DMSO-d_6) δ 4.48 (s, 2H, CH_2), 4.76 (d, 1H, J_{trans} = 17.2 Hz, CH), 5.03 (d, 1H, J_{cis} = 10.4 Hz, CH), 5.83 (m, 1H, CH=), 6.08 (s, 1H, pyrrole H), 6.59 (s, 1H, pyrrole H), 6.64 (s, 1H, CH), 6.84 (s, 1H, imidazole H), 7.10-7.14 (m, 3H, imidazole H and benzene H), 7.30-7.37 (m, 6H, benzene H), 7.62 (s, 1H, imidazole H). Anal. Calcd for $C_{23}H_{19}Cl_2N_3$: C, 67.65; H, 4.69; N, 10.29; Cl, 17.37%. Found C, 67.75; H, 4.70; N, 10.28; Cl, 17.40%.

1-[[1-(4-Nitrophenyl)-1*H*-pyrrol-3-yl](phenyl)methyl]-1*H*-imidazole (7a). Compound **7a** was prepared from **22a** by means of GP-A**.** 71% as yellow-orange oil; 15 h ; chloroform; IR ν 1520, 1335 (NO_2) cm^{-1}. ^{1}H NMR (Acetone-d_6) δ 6.33 (s, 1H, pyrrole C4-H), 6.70 (s, 1H, CH), 6.95 (s, 1H, imidazole H), 7.11 (s, 1H, imidazole H), 7.26-7.39 (m, 6H, benzene H and pyrrole C5-H), 7.53 (s, 1H, pyrrole C2-H), 7.62 (s, 1H,

imidazole H), 7.81 (d, 2H, benzene H), 8.30 (d, 2H, benzene H). Anal. Calcd for $C_{20}H_{16}N_4O_2$: C, 69.76; H, 4.68; N, 16.27%. Found C, 69.70; H, 4.69; N, 16.32%.

1-[(4-Nitrophenyl)[1-(4-nitrophenyl)-1*H*-pyrrol-3-yl]methyl]-1*H*-imidazole (7b). Compound **7b** was prepared from **22b** by means of GP-A**.** 58% as yellow solid; 181-182 °C; ethanol; 16h; ethyl acetate; IR ν 1508, 1332 (NO_2) cm^{-1}. ^1H NMR (Acetone-*d*$_6$) δ 6.40 (q, 1H, pyrrole C4-H), 6.94 (s, 1H, CH), 7.00 (s, 1H, imidazole H), 7.19 (s, 1H, imidazole H), 7.42 (t, 1H, pyrrole C5-H), 7.50 (d, 2H, benzene H), 7.58 (dd, 1H, pyrrole C2-H), 7.69 (s, 1H, imidazole H), 7.84 (d, 2H, benzene H), 8.24 (d, 2H, benzene H), 8.33 (d, 2H, benzene H). Anal. Calcd for $C_{20}H_{15}N_5O_4$: C, 61.69; H, 3.88; N, 17.99%. Found C, 61.77; H, 3.87; N, 17.91%.

1-[(4-Chlorophenyl)[1-(4-nitrophenyl)-1*H*-pyrrol-3-yl]methyl]-1*H*-imidazole (7c). Compound **7c** was prepared from **22c** by means of GP-A**.** 61% as brown oil; 40 min; chloroform; IR ν 1530,1340 (NO_2) cm^{-1}. ^1H NMR (Acetone-*d*$_6$) δ 6.35 (s, 1H, pyrrole C4-H), 6.74 (s, 1H, CH), 6.96 (s, 1H, imidazole H), 7.13 (s, 1H, imidazole H), 7.27 (d, 1H, benzene H), 7.34 (s, 1H, pyrrole C5-H), 7.40 (d, 1H, benzene H), 7.55 (t, 1H, pyrrole C2-H), 7.65 (s, 1H, imidazole H), 7.83 (d, 2H, benzene H), 8.32 (d, 2H, benzene H). Anal. Calcd for $C_{20}H_{15}ClN_4O_2$: C, 63.41; H, 3.99; N, 14.79; Cl, 9.36%. Found C, 63.56; H, 3.98; N, 14.81; Cl, 9.37%.

1-[(4-Chlorophenyl)[1-[4-(trifluoromethyl)phenyl]-1*H*-pyrrol-3-yl]methyl]-1*H*-imidazole (7d). Compound **7d** was prepared from **22d** by means of GP-A. 100% as green oil; 15 h ; chloroform; IR ν 1330 (CF_3) cm^{-1}. ^1H NMR (Acetone-d_6) δ 6.31 (s, 1H, pyrrole C4-H), 6.73 (s, 1H, CH), 6.97 (s, 1H, imidazole H), 7.13 (s, 1H, imidazole H), 7.25-7.28 (m, 3H, benzene H and pyrrole C5-H), 7.40 (d, 2H, benzene H), 7.47 (t, 1H, pyrrole C2-H), 7.66 (s, 1H, imidazole H), 7.77 (m, 4H, benzene H). Anal. Calcd for $C_{21}H_{15}ClF_3N_3$: C, 62.77; H, 3.76; N, 10.46; Cl, 8.82; F, 14.18%. Found C, 62.70; H, 3.75; N, 10.45; Cl, 8.81; F, 14.16%.

4-[[1-(4-Chlorophenyl)-1*H*-pyrrol-3-yl](1*H*-imidazol-1-yl)methyl]benzonitrile (7e). Compound **7e** was prepared from **22e** by means of GP-A. 49% as brown oil; 100 min; ethyl acetate; IR ν 2230 (CN) cm^{-1}. ^1H NMR (Acetone-d_6) δ 6.28 (t, 1H, pyrrole C4-H), 6.83 (s, 1H, CH), 6.98 (s, 1H, imidazole H), 7.14 (s, 1H, imidazole H), 7.19 (t, 1H, pyrrole C5-H), 7.39 (t, 1H, pyrrole C2-H), 7.40 (d, 2H, benzene H), 7.47 (d, 2H, benzene H), 7.55 (d, 2H, benzene H), 7.67 (s, 1H, imidazole H), 7.77 (d, 2H, benzene H). Anal. Calcd for $C_{21}H_{15}ClN_4$: C, 70.29; H, 4.21; N, 15.61; Cl, 9.88%. Found C, 70.31; H, 4.22; N, 15.59; Cl, 9.87%.

4-[3-[(4-Cyanophenyl)(1*H*-imidazol-1-yl)methyl]-1*H*-pyrrol-1-yl]benzonitrile (7f). Compound **7f** was prepared from **22f** by means of GP-A. 20% as yellow solid ; 184-

185°C; ethanol ; 2h; ethyl acetate IR ν 2232 (CN) cm^{-1}. ^1H NMR (Acetone-d_6) δ 6.36 (q, 1H, pyrrole C4-H), 6.86 (s, 1H, CH), 6.98 (t, 1H, imidazole H), 7.16 (t, 1H, imidazole H), 7.35 (t, 1H, pyrrole C5-H), 7.42 (d, 2H, benzene H), 7.53 (dd, 1H, pyrrole C2-H), 7.67 (s, 1H, imidazole H), 7.77-7.81 (m, 4H, benzene H), 7.87 (d, 2H, benzene H). Anal. Calcd for $C_{22}H_{15}N_4$: C, 75.63; H, 4.33; N, 20.04%. Found C, 75.67; H, 4.34; N, 19.99%.

1-[[4-(*tert*-Butyl)phenyl][1-(4-chlorophenyl)-1*H*-pyrrol-2-yl]methyl]-1*H*-imidazole (8a). Compound **8a** was prepared from **21a** by means of GP-A. 66% as yellow solid; 182-183 °C; cyclohexane; 1h; ethyl acetate: *n*-hexane 2:1; ^1H NMR (DMSO-d_6) δ 1.17 (s, 9H, CH_3), 5.66 (s, 1H, pyrrole H), 6.13 (s, 1H, pyrrole H), 6.55 (s, 1H, CH), 6.74 (s, 1H, imidazole H), 6.80 (s, 1H, imidazole H), 6.89 (s, 1H, pyrrole H), 6.95 (d, 2H, benzene H), 7.12 (d, 2H, benzene H), 7.26-7.27 (m, 3H, benzene H and imidazole H), 7.35 (d, 2H, benzene H). Anal. Calcd for $C_{24}H_{24}ClN_3$: C, 73.93; H, 6.20; N, 10.78; Cl, 9.09%. Found C, 73.97; H, 6.21; N, 10.79; Cl, 9.12%.

1-[[1-(4-Chlorophenyl)-1*H*-pyrrol-2-yl](2,4-dichlorophenyl)methyl]-1*H*-imidazole (8b). Compound **8b** was prepared from **21b** by means of GP-A. 89% as orange solid; 129-130 °C; cyclohexane; 105 min; chloroform; ^1H NMR (DMSO-d_6) δ 5.66 (s, 1H, pyrrole H), 6.13 (s, 1H, pyrrole H), 6.59 (d, 1H, benzene H), 6.63 (s, 1H, CH), 6.86 (s, 1H,

imidazole H), 6.91 (s, 1H, imidazole H), 6.96 (s, 1H, pyrrole H), 7.05 (d, 2H, benzene H), 7.34 (d, 1H, benzene H), 7.40-7.42 (m, 3H, benzene H), 7.54 (s, 1H, imidazole H). Anal. Calcd for $C_{20}H_{14}Cl_3N_3$: C, 59.65; H, 3.50; N, 10.43; Cl, 26.41%. Found C, 59.57; H, 3.49; N, 10.41; Cl, 26.31%.

1-[[1-(2,4-Dichlorophenyl)-1*H*-pyrrol-2-yl](2,4-dichlorophenyl)methyl]-1*H*-imidazole (8c). Compound **8c** was prepared from **21a** by means of GP-A. 73% as brown oil; 15 h ; ethyl acetate: *n*-hexane 1:1; ^{1}H NMR ($CDCl_3$) δ 5.84 (s, 1H, pyrrole H), 5.91 (s, 1H, pyrrole H), 6.24 (d, 1H, benzene H), 6.37 (s, 1H, CH), 6.45 (s, 1H, imidazole H), 6.70-6.82 (m, 4H, imidazole H, pyrrole H and benzene H), 7.13-7.27 (m, 2H, benzene H), 7.35 (d, 1H, benzene H), 7.47 (s, 1H, imidazole H). Anal. Calcd for $C_{20}H_{13}Cl_4N_3$: C, 54.95; H, 3.00; N, 9.61; Cl, 32.44%. Found C, 54.90; H, 3.01; N, 9.62; Cl, 32.37%.

Synthesis of 4-chloro-2-(thiophen-2-yl)benzaldheyde (9f). $Pd(dba)_2$ (0.05 g, 0.09 mmol) and PCy_3 (0.05 g, 0.16 mol) were added into a vial under magnetical stirring and purged with argon atmosphere for 10 minutes to form the $Pd(dba)_2/PCy_3$ complex. Thiophen-2-ylboronic acid (0.5 g, 2.86 mmol), $K_2PO_4{\cdot}H_2O$ (1.73 g, 7.8 mmol), DMF (3 mL) and the commercially available 2,4-dichlorobenzaldheyde (3 mmol) were added onto the vial under argon atmosphere. The vial was placed into

the microwave cavity (80 °C, 100 W, 100 PSI, 1 h). The reaction mixture was poured into H_2O and extracted with ethyl acetate. The combined organic phases were washed with brine, dried over Na_2SO_4, evaporated under reduced pressure to obtain 1.5 g of crude **9f** as brown oil. The raw material composed by a mixture of derivatives **9f**, **9j** and **9k** was purified by column chromatography (silica gel/ petroleum ether: chloroform 2:1 as eluent) to furnish the derivative **9f** in mixture with its 4-chloro isomer **9j**. Yield (%), melting point (°C), recrystallization solvent, IR, ^{1}H-NMR and elemental analysis data are reported in Supporting Information.

Synthesis of 1-chloro-4-(isocyano(tosyl)methyl)benzene (13). To a cooled suspension of **17** (2.0 g, 6.2 mmol) in 12 mL of DME was added dropwise in 5 minutes $POCl_3$ (1.4 mL) and then in 10 minutes a solution of triethylamine (4.3 mL) in 3.1 mL of DME. The reaction was stirred at -5 °C for 45 minutes, pured into $NaHCO_3$ saturated solution (62 mL). The formed solid was filtered and washed with water, solved in DCM and dried over Na_2SO_4 anhydrous obtaining 2.10 g of crude **13** as brown solid. Crude **13** was purified by column chromatography (silica gel/ ethyl acetate) to furnish pure **13** (91%; m.p. 108-110 °C; recrystallized from cyclohexane). Spectroscopic data are reported in literature[40].

Synthesis of (4-chlorophenyl)[5-(4-chlorophenyl)-1*H*-pyrrol-3-yl]methanone (14). To a suspension of NaH 60% (6.5 g, 160 mmol) in 205 mL of anhydrous diethyl ether under argon stream was added dropwise a solution of 3-chloro-1-(4-chlorophenyl)propan-1-one (10 g, 49 mmol) and **13** (16.5 g, 54 mmol) in diethyl ether/DMSO 2:1 (615 mL) at room temperature. The reaction mixture was stirred at room temperature for 50 min, diluted with water and extract with ethyl acetate. The combined organic phases was washed with brine, dried over Na_2SO_4 and evaporated at reduced pressure to obtained crude product **14** as brown solid. Crude **14** was purified by column chromatography (aluminum oxide/ ethyl acetate: chloroform 1:1) to furnish pure **14** as yellow solid (33%; m.p. 229-231 °C; recrystallized from toluene). IR, ^{1}H-NMR and elemental analysis data are reported in Supporting Information.

Synthesis of *N*-[(4-chlorophenyl)(tosyl)methyl]formamide (17). A mixture of 4-chlorobenzaldehyde (6 g, 43 mmol), *p*-toluenesulfinic acid (10.15 g, 65 mmol), formamide (4.95 g, 110 mmol), and TMSCl (5.11 g, 47 mmol) in toluene/acetonitrile 1:1 (46 mL) were stirred at 50 °C for 5 h. The mixture was cooled at 0 °C, diluted with *i*PrOH (21 mL) and water (85 mL), and stirred for 30 min. The solid that formed was filtered and washed with petroleum ether obtaining 10.5 g of **17** as white solid

(80%; m.p. 118-120 °C; recrystallized from benzene). Spectroscopic data are reported in literature.[40]

Biological methods. *In vitro antiprotozoal assay*. The *in vitro* activities against *T. b. rhodesiense*, *T. cruzi*, *L. donovani*, and *P. falciparum* (K1 strain) and cytotoxicity assessment using L6 cells (rat skeletal myoblasts) were determined as previously described.[50] The following strains, parasite forms and reference drugs were used: *T. b. rhodesiense*, STIB900, trypomastigote form, melarsoprol (MEL); *T. cruzi*, Tulahuen C2C4, amastigote form in L6 rat myoblasts, Bz; *L. donovani*, MHOM/ET/67/L82, axenic amastigote form, miltefosine (MF); *P. falciparum*, K1 (chloroquine and pyrimethamine resistant strain) erythrocytic stage, chloroquine (CHQ).

UV-vis binding assay in 96-well format. Compounds **5i**, **6a-c** and **8b** were tested for binding to TcCYP51 in a 96-well plate using Multiskan Go Microplate spectrophotometer (Thermo-Scientific). TcCYP51 was obtained as previously described.[51] Purified TcCYP51 was diluted to 5 μM in 50 mM phosphate buffer (pH 7.4) and 10% glycerol buffer. Two hundred microliters of either protein or buffer alone was dispensed into wells of the 96-well plate. To each well, either 5 μM or 10 μM of each compound dissolved in DMSO was added and mixed with the protein solution or the buffer blank. A protein blank was made up by adding the equivalent volume of buffer, instead of compound or DMSO. Spectra of each well were recorded at 25 °C between 350 nm and 500 nm. Spectra of the respective buffer-compound and protein-buffer blanks were subtracted from the spectra of protein-compound samples. These difference spectra were plotted and interpreted based on the positions of a peak and a trough.

UV-vis spectroscopy in 1-cm quartz split chamber cuvette. Spectra were recorded using a Cary 1 E (Varian) dual beam UV-visible spectrophotometer. Spectral binding titrations were performed in the split chamber tandem spectrophotometer cuvette at 25 °C. Compound **6a** was dissolved in

DMSO. For each titration, 2 ml of 2 μM TcCYP51 in 20 mM potassium phosphate, pH 7.4, was titrated in the split chamber sample cuvettes with the inhibitor being added in 500 nM increments. After each addition, the cuvette was inverted multiple time to facilitate inhibitor distribution to both chambers. To compensate for the **6a** own absorbance, 1 mL of 4 μM TcCYP51 was added to one chamber of the reference cuvette, while 1 ml of buffer alone was added to the adjacent chamber. **6a** was titrated into the buffer-containing chamber and was mixed-in by pipetting to avoid contamination of the protein compartment.

Spectra were recorded from 350 to 500 nm. A binding isotherm for **6a** was generated by plotting the difference between the absorbance minimum at 388 nm and the absorbance maximum at 426 nm as a function of drug concentration. The spectral dissociation constant, K_D, was extrapolated using the Curve Fitting Tool in MATLAB (MathWorks, Natick, MA) by fitting the binding isotherm using the quadratic Morrison equation $\Delta A = (\Delta A_{max} / 2[E])((K_D + [L] + [E]) - ((K_D + [E] + [L])^2 - 4[E][L])^{0.5})$, where ΔA is the difference between absorbance maximum and minimum, ΔA_{max} is the extrapolated maximum absorbance difference, [L] is the ligand concentration and [E] is the enzyme concentration.

Inhibition of human CYPs in vitro assay. CYP450 screening systems were based on bioluminescent detection technique where the activity of firefly luciferase is coupled to the metabolism of pro-luciferin substrates (P450-Glo™ Assays, Promega Corporation) as reported in Figure S1 Supporting Information. The substrates used for each isoform are shown in Table S5 Supporting Information while the IC_{50} values for tested compounds and positive controls used are reported in Table 3. All incubations were performed in a single plate format at 37°C. Incubation contained phosphate buffer, microsomal protein (variable concentration depending on the assay), appropriate substrate (at the approximate K*m* value) and either solvent vehicle or test compound. All incubations were initiated by adding NADPH. The total amount of organic solvent was <1%. Since significant inhibition was observed as a result of this screen, an IC_{50} value was derived from the dose-response profiles for the specific CYP450

reaction(s). IC_{50} values were determined through nonlinear regression curve fitting analysis, with the software program XLfit 5.2.0.0 (IDBS LtD).

In vivo T. cruzi assay- Parasites. Transgenic *T. cruzi* CL Brener parasites expressing a red-shifted luciferase that emits light in the tissue-penetrating orange-red region of the spectrum was a gift from Dr. John Kelly, London School of Hygiene and Tropical Medicine, London, United Kingdom.[52]

In vivo T. cruzi assay- Animals. In vivo experiments were performed at the University of California San Diego (UCSD), La Jolla, California, USA. Six weeks old female BALB/c mice weighting 18-20 g were purchased from Jackson Laboratories (Farmington, CT, USA). Mice were housed in a maximum number of 5 animals per cage and kept in a conventional room at 20-24 °C under a 12 h/12 h light/dark cycle. The animals were provided with sterilized water and chow ad libitum.

In vivo T. cruzi assay- Infection and Treatment. Mice were infected by intraperitoneal injection with 10^4 *T. cruzi* CL Brener trypomastigotes prepared as described elsewhere.[23] Only mice with detectable luminescence at day 3 post-infection were used for treatment. Compounds **6a**, **6b** and **8b** were administered for 4 days intraperitoneally at 25 mg/kg b. i.d. as a 10% solution in Kolliphor HS 15 (Sigma no. 42966), also known as solutol. Two control groups included vehicle control, which received 10% solutol, and the positive control group, which received Bz, 50 mg/kg, both b.i.d., i. p.

In vivo T. cruzi assay- Bioluminescent Imaging. BALB/c mice infected with parasites carrying a bioluminescent marker were imaged before treatment (3 days post-infection) and after 4 days of treatment (7 days post injection) as previously described.[27] Briefly, mice were injected i. p. with 150 mg/kg D-luciferin potassium salt in PBS (Gold Biotechnology, St. Louis, MO), and 5 min later, anesthetized by isofluorane inhalation (3e5%) and imaged using IVIS Lumina *in vivo* imaging system (Perkin Elmer, Waltham, MA) with 180s exposure time. Data acquisition and analysis were performed with the LivingImage V4.1 software (Perkin Elmer, Waltham, MA). Uninfected controls were imaged in parallel to establish a negative threshold. The absolute numbers of photons/s/cm^2 were measured in all five mice in each group and compared directly between compound-treated mice and the control groups. Two-tailed paired Student t-test was used to assess statistical significance between

luminescence values of vehicle-treated and compound-treated groups at day 7 post-infection; values are statistically significant when $p \leq 0.05$.

Ethics Statements. Research performed at UC San Diego was conducted in compliance with the Animal Welfare Act and other federal statutes and regulations relating to animals and experiments involving animals and adheres to the principles stated in the Guide for the Care and Use of Laboratory Animals, National Research Council, 2011. The facility where this research was conducted is fully accredited by the Association for Assessment and Accreditation of Laboratory Animal Care International. Animal research was conducted under approved protocol S14187 from the Institutional Animal Care and Use Committee, University of California, San Diego. Euthanasia was accomplished by CO_2 inhalation or by sodium pentobarbital overdose (60 mg/kg), followed by cervical dislocation. These methods of euthanasia have been selected because they cause minimal pain and distress to animals, are relatively quick, and do not adversely impact interpretation of the results of studies. All methods are in accord with the recommendations of the Panel on Euthanasia of the American Veterinary Medical Association.

Enantiomer separation of 4. *HPLC resolution of 4.* HPLC enantioseparation of **4** was performed by using the stainless-steel Chiralcel OD (250 mm x 4.6 mm i.d. and 250 x 10 mm i.d.) (Chiral Technologies Europe, Illkirch, France) columns. All chemicals solvents for HPLC were purchased from Aldrich (Italy) and used without further purification. The analytical HPLC apparatus consisted of a Perkin-Elmer (Norwalk, CT, USA) 200 lc pump equipped with a Rheodyne (Cotati, CA, USA) injector, a 20-μL sample loop, a HPLC Dionex CC-100 oven (Sunnyvale, CA, USA) and a Jasco (Jasco, Tokyo, Japan) Model CD 2095 Plus UV/CD detector. For

semipreparative separations a Perkin-Elmer 200 LC pump equipped with a Rheodyne injector, a 1 mL sample loop, a Perkin-Elmer LC 101 oven and Waters 484 detector (Waters Corporation, Milford, MA, USA) were used. The signal was acquired and processed by Clarity software (DataApex, Prague, The Czech Republic).

Circular dichroism. The circular dichroism (CD) spectra were measured by using a Jasco Model J-700 spectropolarimeter. The optical path and temperature were set at 0.1 mm and 20°C, respectively. The spectra are average computed over three instrumental scans and the intensities are presented in terms of ellipticity values (mdeg).

Polarimetry. Specific rotations were measured at 589 nm by a PerkinElmer polarimeter model 241 equipped with a Na/Hg lamp. The volume of the cell was 1 cm^3 and the optical path was 10 cm. The system was set at 20 °C.

*Crystal structure determination for compound (R)-(-)-**4**.* $2x(C_{20}H_{14}N_3Cl_3)+O$, M=821.38, Monoclinic, space group P 2_1, *a*=11.967(5), *b*=7.646(2), *c*=21.750(9)Å, β=93.51(4), V=1986(1)$Å^3$, Z=2 D_c=1.373, μ=4.269mm^{-1}, F(000)= 840. 6532 reflections were collected with a 4.11<θ< 63.19 range with a completeness to theta 93.9%; 4249 were unique, the Goodness-of-fit on F^2 was 1.017; the parameters were 479 and the final R index was 0.1061 for reflections having I>2σI. A colourless prismatic shaped

crystal (0.08x0.07x0.03) was used for data collection. Asymmetric unit contains two molecules and a water co-crystallized.

Hydrogen atoms were assigned in calculated positions, except for the two on oxygen of solvent and the one on N3, whose position were not assignable. They were impossible to find in the Fourier difference map too.

RX-analysis was carried out with a Goniometer Oxford Diffraction KM4 Xcalibur2 at room temperature. Cu/Kα radiation (40mA/-40KV), monochromated by an Oxford Diffraction Enhance ULTRA assembly, and an Oxford Diffraction Excalibur PX Ultra CCD were used for cells parameters determination and data collection.

The integrated intensities, measured using the ω scan mode, were corrected for Lorentz and polarization effects.[53]

Direct methods of SIR2004[54] were used in solving the structures and they were refined using the full-matrix least squares on F^2 provided by SHELXL97.[55]

Multi-scan symmetry-related measurement was used as experimental absorption correction type.

The non-hydrogen atoms were refined anisotropically whereas hydrogen atoms were refined as isotropic.

The X-ray CIF file for this structure has been deposited at the Cambridge Crystallographic Data Center and allocated with the deposition number CCDC 1030509.

Copies of the data can be obtained, free of charge, from CCDC, 12 Union Road, Cambridge, CB2 1EZ UK (e-mail: deposit@ccdc.cam.ac.uk; internet://www.ccdc.cam.ac.uk).

ASSOCIATED CONTENT

Supporting Information. The Supporting Information is available free of charge on the ACS Publications website at DOI:

Chemical and physical data of derivatives **9a-k, 10a-j, 11a-j, 12a-j, 15b,c, 16a-c, 18a-e, 19a-c, 20a-f, 21a-c, 22a-f**, spectroscopic data, elemental analysis and some reaction data of derivatives **9f,j,k, 10b,c,e-j, 11a-j, 12a-j, 14, 15b,c, 16a-c, 19a-c, 20a-f, 21a-c, 22a-f,** atomic coordinates and equivalent isotropic displacement parameters of (*R*)-(-)-**4** X-ray structure, bond lengths and angles of (*R*)-(-)-**4** X-ray

structure, anisotropic displacement parameters of (*R*)-(-)-**4** X-ray structure, the P450-Glo™ assay reaction scheme, P450-Glo™ luminogenic substrate used in the assay

Molecular formula strings and some data (CSV).

AUTHOR INFORMATION

Corresponding Author

∗Phone: +39-06-49693247. E-mail: roberta.costi@uniroma1.it

ORCID

Francesco Saccoliti: 0000-0002-2907-5503

Valentina Noemi Madia: 0000-0002-5724-612X

Valeria Tudino: 0000-0001-9024-9835

Luca Pescatori: 0000-0003-4734-7856

Antonella Messore: 0000-0003-0158-5816

Daniela De Vita: 0000-0002-0370-4244

Luigi Scipione: 0000-0002-2006-7005

Marcel Kaiser: 0000-0003-1785-7302

Pascal Mäser: 0000-0003-3122-1941

Claudia M. Calvet: 0000-0003-1275-1226

Gareth K. Jennings: 0000-0001-7986-8491

Larissa M. Podust: 0000-0002-8537-8760

Giacomo Pepe: 0000-0002-7561-2023

Roberto Cirilli: 0000-0001-6346-1953

Cristina Faggi: 0000-0002-2448-6354

Roberta Costi: 0000-0002-1314-9029

Roberto Di Santo: 0000-0002-4279-7666

Author Contributions

The manuscript was written through contributions of all authors. All authors have given approval to the final version of the manuscript.

Notes

The authors declare no competing financial interest.

ACKNOWLEDGMENTS

The authors thank Diane Thomas and Jair Lage Siqueira Neto for support in animal studies. This work was supported by the UCSD start up fund to L.M.P; the "Sapienza" University of Rome to L.S., R.C. and R.D.S. (Ateneo 2015 C26H15WYPW and Ateneo 2016 RM116154C9A02AC1).

ABBREVIATIONS USED

CYP51, sterol 14α-demethylase; TcCYP51, *Trypanosoma cruzi* CYP51; VL, visceral leishmaniasis; HAT, human African trypanosomiasis; SAR, structure−activity relationship; CDI, *N,N*-carbonyldiimidazole; TosMIC, toluene-4-sulfonylmethylisocyanide; TMSCl, trimethylsilyl chloride; DMSO, dimethyl sulfoxide; THF, tetrahydrofuran; DMF, *N,N*-dimethylformamide; DME, dimethoxyethane; DCM, dichloromethane; Tb, *Trypanosoma brucei rhodesiense*; Tc, *Trypanosoma cruzi*; Ld, *Leishmania donovani*; Pf, *Plasmodium falciparum*; MEL, melarsoprol; Bz, benznidazole; MF, miltefosine; CHQ, chloroquine; ART, artemisinin; PPT, podophyllotoxin; Ph, phenyl; Py, 1-pyrrolyl; Tioph, 2-thienyl; Np, naphtyl; GP, general procedure; IR, infrared.

REFERENCES

1. Field, M. C.; Horn, D.; Fairlamb, A. H.; Ferguson, M. A. J.; Gray, D. W.; Read, K. D.; De Rycker, M.; Torrie, L. S.; Wyatt, P. G.; Wyllie, S.; Gilbert, I. H. Anti-trypanosomatid drug discovery: an ongoing challenge and a continuing need. *Nat. Rev. Microbiol.* **2017**, *15*, 217-231.

2. WHO, Fact sheets malaria. http://www.who.int/news-room/fact-sheets/detail/malaria (accessed July 3, 2018).

3. Cavalli, A.; Bolognesi, M.L. Neglected tropical diseases: multi-target-directed ligands in the search for novel lead candidates against Trypanosoma and Leishmania. *J. Med. Chem.* **2009**, *52*, 7339-7359

4. Bernardes, L. S.; Zani, C. L.; Carvalho, I. Trypanosomatidae diseases: from the current therapy to the efficacious role of trypanothione reductase in drug discovery. *Curr. Med. Chem.* **2013**, *20*, 2673-2696.

5. WHO, Neglected tropical diseases. http://www.who.int/neglected_diseases/diseases/en/ (accessed July 3, 2018).

6. Lee, B. Y; Bartsch, S. M.; Gorham, K. M. Economic and financial evaluation of neglected tropical diseases. *Adv. Parasitol.* **2015**, *87*, 329-417.

7. Lepesheva, G. I.; Hargrove, T. Y.; Rachakonda, G.; Wawrzak, Z.; Pomel, S.; Cojean, S.; Nde, P. N.; Nes, W. D.; Locuson, C.W.; Calcutt, M. W.; Waterman, M. R.; Daniels, J. S.; Loiseau, P. M.; Villalta, F. VFV as a new effective CYP51 structure-derived drug candidate for Chagas disease and visceral leishmaniasis. *J. Infect. Dis*. **2015**, *212*, 1439-1448.

8. WHO, Fact sheets Leishmaniasis. http://www.who.int/en/news-room/fact-sheets/detail/leishmaniasis (accessed July 3, 2018)

9. Saccoliti, F.; Angiulli, G.; Pupo, G.; Pescatori, L.; Madia, V. N.; Messore, A.; Colotti, G.; Fiorillo, A.; Scipione, L.; Gramiccia, M.; Di Muccio, T.; Di Santo, R.; Costi, R.; Ilari, A. Inhibition of *Leishmania infantum* trypanothione reductase by diaryl sulfide derivatives. *J. Enzyme Inhib. Med. Chem*. **2017**, *32*, 304-310.

10. WHO, Fact sheets Chagas disease. http://www.who.int/en/news-room/fact-sheets/detail/chagas-disease-(american-trypanosomiasis)/ (accessed July 3, 2018).

11. WHO, Fact sheets African trypanosomiasis. http://www.who.int/news-room/fact-sheets/detail/trypanosomiasis-human-african-(sleeping-sickness)/ (accessed July 3, 2018).

12. Krauth-Siegel, R. L.; Bauer, H.; Schirmer, R. H. Dithiol proteins as guardians of the intracellular redox milieu in parasites: old and new drug targets in trypanosomes and malaria-causing plasmodia. *Angew. Chem., Int. Ed. Engl.* **2005**, *44*, 690-715.

13. Mäser, P.; Wittlin, S.; Rottmann, M.; Wenzler, T.; Kaiser, M.; Brun, R. Antiparasitic agents: new drugs on the horizon. *Curr. Opin. Pharmacol.* **2012**, *12*, 562-566.

14. Di Santo, R. Natural products as antifungal agents against clinically relevant pathogens. *Nat. Prod. Rep.* **2010**, *27*, 1084-1098.

15. Lepesheva, G. I.; Friggeri, L.; Waterman, M. R. CYP51 as drug targets for fungi and protozoan parasites: past, present and future. *Parasitology* **2018**, 1-17

16. Lepesheva, G. I.; Waterman, M. R. Sterol 14alpha-demethylase (CYP51) as a therapeutic target for human trypanosomiasis and leishmaniasis. *Curr. Top. Med. Chem.* **2011**, *11*, 2060-2071.

17. Choi, J. Y.; Podust, L. M.; Roush, W. R. Drug strategies targeting CYP51 in neglected tropical diseases. *Chem. Rev.* **2014**, *114*, 11242-11271.

18. Docampo, R. Biochemical and ultrastructural alterations produced by miconazole and econazole in *Trypanosoma cruzi*. *Mol. Biochem. Parasitol.* **1981**, *3*, 169-180.

19. Kulkarni M. M; Reddy, N.; Gude, T.; McGwire, B. S. Voriconazole suppresses the growth of Leishmania species *in vitro*. *Parasitol. Res.* **2013**, *112*, 2095-2099.

20. Kaiser, M.; Maser, P.; Tadoori, L. P.; Ioset, J. R.; Brun, R. Antiprotozoal activity profiling of approved drugs: a starting point toward drug repositioning. *PLoS One* **2015**, *10*, e0135556.

21. Buckner, F.; Yokoyama, K.; Lockman, J.; Aikenhead, K.; Ohkanda, J.; Sadilek, M.; Sebti, S.; Van Voorhis, W.; Hamilton, A.; Gelb, M. H. A class of sterol 14-demethylase inhibitors as anti-*Trypanosoma cruzi* agents. *Proc. Natl. Acad. Sci. U.S.A* **2003**; *100*, 15149-15153.

22. Friggeri, L.; Hargrove, T. Y.; Rachakonda, G.; Williams, A. D.; Wawrzak, Z.; Di Santo, R; De Vita, D; Waterman, M. R.; Tortorella, S.; Villalta, F.; Lepesheva, G. I. Structural basis for rational design of inhibitors targeting *Trypanosoma cruzi* sterol 14α -demethylase: two regions of the enzyme molecule potentiate its inhibition. *J. Med. Chem.* **2014**, *57*, 6704−6717.

23. Calvet, C. M.; Choi, J. Y.; Thomas, D.; Suzuki, B.; Hirata, K.; Lostracco-Johnson, S.; de Mesquita L. B.; Nogueira, A.; Meuser-Batista, M.; Silva, T. A.; Siqueira-Neto, J. L.; Roush, W. R.; de Souza Pereira, M. C.; McKerrow, J. H.; Podust, L. M. 4-

Aminopyridyl-based lead compounds targeting CYP51 prevent spontaneous parasite relapse in a chronic model and improve cardiac pathology in an acute model of *Trypanosoma cruzi* infection. *PLoS Negl. Trop. Dis*. **2017,** *11*, e0006132.

24. Guedes-da-Silva, F. H.; Batista, D. G.; Da Silva, C. F.; De Araujo, J. S.; Pavao, B. P.; Simoes-Silva, M. R.; Batista, M. M.; Demarque, K. C.; Moreira, O. C.; Britto, C.; Lepesheva, G. I.; Soeiro, M. N. Antitrypanosomal activity of sterol 14α-demethylase (CYP51) inhibitors VNI and VFV in the Swiss mouse models of Chagas disease induced by the *Trypanosoma cruzi* Y strain. *Antimicrob. Agents Chemother*. **2017**, *61*, e02098.

25. Ferreira de Almeida Fiuza, L.; Peres, R. B.; Simões-Silva, M. R.; da Silva, P. B.; Batista, D. D. G. J.; da Silva C. F.; Nefertiti Silva da Gama, A.; Krishna Reddy, T. R.; Soeiro, M. N. C. Identification of pyrazolo[3,4-e][1,4]thiazepin based CYP51 inhibitors as potential Chagas disease therapeutic alternative: *in vitro* and *in vivo* evaluation, binding mode prediction and SAR exploration. *Eur. J. Med. Chem*. **2018**, *149*, 257-268.

26. Vieira, D.F.; Choi, J. Y.; Calvet, C. M,; Siqueira-Neto, J. L.; Johnston, J. B.; Kellar, D.; Gut, J.; Cameron, M. D.; McKerrow, J. H.; Roush, W. R.; Podust, L. M. Binding

mode and potency of N-indolyloxopyridinyl-4-aminopropanyl-based inhibitors targeting *Trypanosoma cruzi* CYP51. *J. Med. Chem.* **2014**, *57*, 10162-10175.

27. Calvet, C. M,; Vieira, D.F.; Choi, J. Y.; Kellar, D.; Cameron, M. D.; Siqueira-Neto, J. L.; Gut, J.; Johnston, J. B.; Lin, L.; Khan, S.; McKerrow, J. H.; Roush, W. R.; Podust, L. M. 4-Aminopyridyl-based CYP51 inhibitors as anti-*Trypanosoma cruzi* drug leads with improved pharmacokinetic profile and *in vivo* potency. *J. Med. Chem.* **2014**, *57*, 6989-7005.

28. Choi, J. Y.; Calvet, C. M,; Vieira, D.F.; Gunatilleke, S. S.; Cameron, M. D.; McKerrow, J. H.; Podust, L. M.; Roush, W. R. R-Configuration of 4-aminopyridyl-based inhibitors of CYP51 confers superior efficacy against *Trypanosoma cruzi*. *ACS Med. Chem. Lett*. **2014**, *5*, 434-439.

29. Vieira, D.F.; Choi, J. Y.; Roush, W. R.; Podust, L. M. Expanding the binding envelope of CYP51 inhibitors targeting *Trypanosoma cruzi* with 4-aminopyridyl-based sulfonamide derivatives. *ChemBioChem*. **2014**, *15*, 1111-1120.

30. Choi, J. Y.; Calvet, C. M,; Gunatilleke, S. S.; Ruiz, C.; Cameron, M. D.; McKerrow, J. H.; Podust, L. M.; Roush, W. R. Rational development of 4-aminopyridyl-based

inhibitors targeting *Trypanosoma cruzi* CYP51 as anti-chagas agents. *J. Med. Chem.* **2013**, *56*, 7651-7668.

31. Hargrove, T. Y.; Wawrzak, Z.; Alexander, P. W.; Chaplin, J. H.; Keenan, M.; Charman, S. A.; Perez, C. J.; Waterman, M. R.; Chatelain, E.; Lepesheva, G. I. Complexes of Trypanosoma cruzi sterol 14α-demethylase (CYP51) with two pyridine-based drug candidates for Chagas disease: structural basis for pathogen selectivity. *J. Biol. Chem.* **2013**, *288*, 31602-31615.

32. (a) Urbina, J. A. Ergosterol biosynthesis and drug development for Chagas disease. *Mem. Inst. Oswaldo Cruz.* **2009**, *104 Suppl 1*, 311-318. (b) Clayton, J. Chagas disease: pushing through the pipeline. *Nature* **2010**, *465*, S12-15. (c) Urbina, J. A.; Payares, G.; Sanoja, C.; Lira, R.; Romanha, A. J. *In vitro* and *in vivo* activities of ravuconazole on *Trypanosoma cruzi*, the causative agent of Chagas disease. *Int. J. Antimicrob. Agents* **2003**, *21*, 27-38. (d) Molina, I.; Gómez i Prat, J.; Salvador, F.; Treviño, B.; Sulleiro, E.; Serre, N.; Pou, D.; Roure, S.; Cabezos, J.; Valerio, L.; Blanco-Grau, A.; Sánchez-Montalvá, A.; Vidal, X.; Pahissa, A. Randomized trial of posaconazole and benznidazole for chronic Chagas' disease. *N. Engl. J. Med.* **2014**, *370*, 1899-1908. (e) Chatelain, E. Chagas disease drug discovery: toward a new era.

J. Biomol. Screen. **2015**, *20*, 22-35. (f) Urbina, J. A. Recent clinical trials for the etiological treatment of chronic Chagas disease: advances, challenges and perspectives. *J. Eukaryot. Microbiol*. **2015**, *62*, 149-156. (g) Molina, I.; Salvador, F.; Sánchez-Montalvá, A. The use of posaconazole against Chagas disease. *Curr. Opin. Infect. Dis.* **2015**, *28*, 397-407. (h) Morillo, C. A.; Waskin, H.; Sosa-Estani, S.; Del Carmen Bangher, M.; Cuneo, C.; Milesi, R.; Mallagray M.; Apt, W.; Beloscar, J.; Gascon, J.; Molina, I.; Echeverria, L. E.; Colombo, H.; Perez-Molina, J. A.; Wyss, F.; Meeks, B.; Bonilla, L. R.; Gao, P.; Wei, B.; McCarthy, M.; Yusuf, S. STOP-CHAGAS Investigators. Benznidazole and posaconazole in eliminating parasites in asymptomatic *T. cruzi* carriers: the STOP-CHAGAS trial. *J. Am. Coll. Cardiol*. **2017**, *69*, 939-947. (i) Urbina, J. A. Pharmacodynamics and follow-up period in the treatment of human *Trypanosoma cruzi* infections with posaconazole. *J. Am. Coll. Cardiol*. **2017**, *70*, 299-300.

33. (a) Massa, S.; Di Santo, R.; Artico, M.; Costi, R.; Apuzzo, G.; Simonetti, G.; Artico, M. Novel *in vitro* highly active antifungal agents with pyrrole and imidazole moieties. *Med. Chem. Res*. **1992**, *2*, 148-153. (b) Massa, S.; Di Santo, R.; Retico, A.; Costi, R.; Di Filippo, C.; Simonetti, G.; Artico, M. Researches on antibacterial and antifungal

agents. XV. 3-aryl-4-[α-(1*H*-imidazol-1-yl)benzyl]pyrroles with potent antifungal activity. *Eur. Bull. Drug Res*. **1993**, *1*, 12-17. (c) Massa, S.; Di Santo, R.; Costi, R.; Simonetti, G.; Retico, A.; Apuzzo, G.; Artico, M. Antifungal agents. III. Naphthyl and thienyl derivatives of 1*H*-imidazol-1-yl-4-phenyl-1*H*-pyrrol-3-ylmethane. *Farmaco* **1993**, *48*, 725-736. (d) Artico, M.; Di Santo, R.; Costi, R.; Massa, S.; Retico, A.; Apuzzo, G.; Simonetti, G.; Strippoli, V. Antifungal agents. 9. 3-Aryl-4-[α -1(*H*-imidazol-l-yl)arylmethyl]pyrroles: a new class of potent anti-Candida agents. *J. Med. Chem*. **1995**, *38*, 4223-4233. (e) Tafi, A.; Anastassopoulou, J.; Theophanides, T.; Botta, M.; Corelli, F.; Massa, S.; Artico, M.; Costi, R.; Di Santo, R.; Ragno, R. Molecular modeling of azole antifungal agents active against Candida albicans. 1. A comparative molecular field analysis study. *J. Med. Chem.* **1996**, *39*, 1227-1235. (f) Di Santo R, Costi R, Artico M.; Massa, S.; Musiu, C.; Scintu, F.; Putzolu, M.; La Colla, P. Antifungal estrogen-like imidazoles. Synthesis and antifungal activities of thienyl and l*H*-pyrrolyl derivatives of 1-aryl-2-(l*H*-imidazol-1-yl)ethane. *Eur. J. Med. Chem*. **1997**, *32*, 143-149. (g) Tafi, A.; Costi, R.; Botta, M.; Di Santo, R.; Corelli, F.; Massa, S.; Ciacci, A.; Manetti, F.; Artico, M. Antifungal agents. 10. New derivatives of 1-[(aryl)[4-aryl-1*H*-pyrrol-3-yl]methyl]-1*H*-imidazole, synthesis, anti-Candida activity, and quantitative structure-analysis relationship studies. *J. Med. Chem.* **2002**; *45*, 2720-

2732. (h) Di Santo, R.; Tafi, A.; Costi, R.; Botta, M.; Artico, M.; Corelli, F.; Forte, M.; Caporuscio, F.; Angiolella, L.; Palamara, A. T. Antifungal Agents. 11. *N*-Substituted derivatives of 1-[(aryl)(4-aryl-1*H*-pyrrol-3-yl)methyl]-1*H*-imidazole: synthesis, anti-Candida activity, and QSAR studies. *J. Med. Chem.* **2005**, *48*, 5140-5153.

34. Saccoliti, F.; Madia, V. N.; Tudino, V.; De Leo, A.; Pescatori, L.; Messore, A.; De Vita, D.; Scipione, L.; Brun, R.; Kaiser, M.; Mäser, P.; Calvet, C. M.; Jennings, G. K.; Podust, L. M; Costi, R.; Di Santo, R. Biological evaluation and structure-activity relationships of imidazole-based compounds as antiprotozoal agents. *Eur. J. Med Chem.* **2018**, *156*, 53-60.

35. Kobayashi, K.; Himei, Y.; Fukamachy, S.; Tanmatsu, M.; Morikawa, O.; Konishi, H. Synthesis of 9-arylamino- and (*Z*)-9-arylimino-9*H*-pyrrolo-[1,2-*a*]indoles by reactions of 2-(pyrrol-1-yl)-benzaldehydes with arylamines. *Tetrahedron* **2007**, *63*, 4356-44359.

36. Inada, K.; Miyaura, N. Synthesis of biaryls via cross-cupling reaction of arylboronic acids with aryl chlorides catalyzed by $NiCl_2$/triphenylphosphine complexes. *Tetrahedron* **2000**, *56*, 8657-8660.

37. Kodomari, M.; Satoh, H.; Yoshitomi, S. Selective halogenation of aromatic hydrocarbons with alumina-supported copper (II) halides. *J. Org. Chem.* **1988**, *53*, 2093-2094.

38. Dinesha; Viveka, S.; Priya, B. K.; Pai, K. S.; Naveen, S.; Lokanath, N.K.; Nagaraja, G. K. Synthesis and pharmacological evaluation of some new fluorine containing hydroxypyrazolines as potential anticancer and antioxidant agents. *Eur. J. Med Chem.* **2015**, *104*, 25-32.

39. Zhang, H.; Jin, H.; Ji, L. Z.; Tao, K.; Liu, W.; Zhao, H. Y.; Hou, T. P. Design, synthesis, and bioactivities screening of a diaryl ketone-inspired pesticide molecular library as derived from natural products. *Chem. Biol. Drug. Des.* **2011**, *78*, 94-100.

40. Chaudhary, A.; Sharma, P. P.; Bhardwaj, G.; Jain, G.; Bharatam, P. V.; Shrivastav, B.; Roy. R. K. Synthesis, biological evaluation, and molecular modeling studies of novel heterocyclic compounds as anti-proliferative agents. *Med. Chem. Res.* **2013**, *22*, 5654-5669.

41. Ma, H. C.; Jiang, X. Z. *N*-hydroxyimides as efficient ligands for the copper-catalyzed *N*-arylation of pyrrole, imidazole, and indole. *J. Org. Chem.* **2007**, *72*, 8943-8946.

42. Shen, T.; Wang, T.; Qin, C.; Jiao, N. Silver-catalyzed nitrogenation of alkynes: a direct approach to nitriles through C≡C bond cleavage. *Angew. Chem., Int. Ed. Engl.* **2013**, *52*, 6677-6680.

43. Azizi, N.; Khajeh-Amiri, A.; Ghafuri, H.; Bolourtchian, M.; Reza Saidi M. Iron-catalyzed inexpensive and practical synthesis of N-substituted pyrroles in water. *Synlett* **2009**, *14*, 2245-2248.

44. Rodrigues, J. R.; Lourenco, D.; Gamboa, N. Disturbance in hemoglobin metabolism and *in vivo* antimalarial activity of azole antimycotics, *Rev. Inst. Med. Trop. Sao Paulo*. **2011**, *53*, 25-29.

45. Huy, N. T.; Kamei, K.; Kondo, Y.; Serada, S.; Kanaori, K.; Takano, R.; Tajima, K.; Hara, S. Effect of antifungal azoles on the heme detoxification system of malarial parasite. *J. Biochem.* **2002**, *131*, 437-444.

46. Yadav, N.; Agarwal, D.; Kumar, S.; Dixit, A. K.; Gupta, R. D.; Awasthi, S. K. *In vitro* antiplasmodial efficacy of synthetic coumarin-triazole analogs. *Eur. J. Med. Chem.* **2018**, *145*, 735-745.

47. Balabadra, S.; Kotni, M.; Manga, V.; Allanki, A. D.; Prasad, R.; Sijwali, P. S. Synthesis and evaluation of naphthyl bearing 1,2,3-triazole analogs as antiplasmodial agents, cytotoxicity and docking studies, *Bioorg. Med. Chem.* **2017**, *25*, 221-232.

48. Devender, N.; Gunjan, S.; Chhabra, S.; Singh, K.; Pasam, V. R.; Shukla, S. K.; Sharma, A.; Jaiswal, S.; Singh, S. K.; Kumar, Y.; Lal, J.; Trivedi, A. K.; Tripathi, R.; Tripathi, R. P. Identification of β-amino alcohol grafted 1,4,5 trisubstituted 1,2,3-triazoles as potent antimalarial agents. *Eur. J. Med. Chem.* **2016**, *109*, 187-198.

49. Luthra, A.; Denisov, I. G.; Sligar, S. G. Spectroscopic features of cytochrome P450 reaction intermediates, *Arch. Biochem. Biophys.* **2011**, *507*, 26-35.

50. Orhan, I.; Sener, B.; Kaiser, M.; Brun, R.; Tesdemir, D. Inhibitory activity of marine sponge-derived natural products against parasitic protozoa. *Mar. Drugs.* **2010**, *8*, 47−58.

51. Chen, C. K.; Leung, S.S.; Guilbert, C.; Jacobson, M. P.; McKerrow, J. H.; Podust, L. M. Structural characterization of CYP51 from *Trypanosoma cruzi* and *Trypanosoma brucei* bound to the antifungal drugs posaconazole and fluconazole. *PLoS Negl. Trop. Dis.* **2010**, *4*, e651.

52. Lewis, M. D.; Fortes Francisco, A.; Taylor, M. C.; Burrell-Saward, H.; McLatchie, A. P.; Miles, M. A.; Kelly, J. M. Bioluminescence imaging of chronic *Trypanosoma cruzi* infections reveals tissue-specific parasite dynamics and heart disease in the absence of locally persistent infection. *Cell. Microbiol.* **2014**, *16*, 1285-1300

53. Walker, N.; Stuart, D.; An empirical method for correcting diffractometer data for absorption effects. *Acta Cystallogr. Sect. A* **1983**, *39*, 158-166.

54. Burla, M. C.; Caliandro, R.; Camalli, M.; Carrozzini, B.; Cascarano, G. L.; De Caro, L.; Giacovazzo, C.; Polidori, G.; Spagna, R. SIR2004: an improved tool for crystal structure determination and refinement. *J. Appl. Cryst.* **2005**, *38*, 381-388.

55. Sheldrick, G, M. SHELXL97: Program for Crystal Structure Refinement; Institut für Anorganische Chemie de Universitat Göttingen: Göttingen, Germany, 1997

Table of Contents graphic